CZECH TECHNICAL UNIVERSITY IN PRAGUE

Faculty of Electrical Engineering

BACHELOR'S THESIS

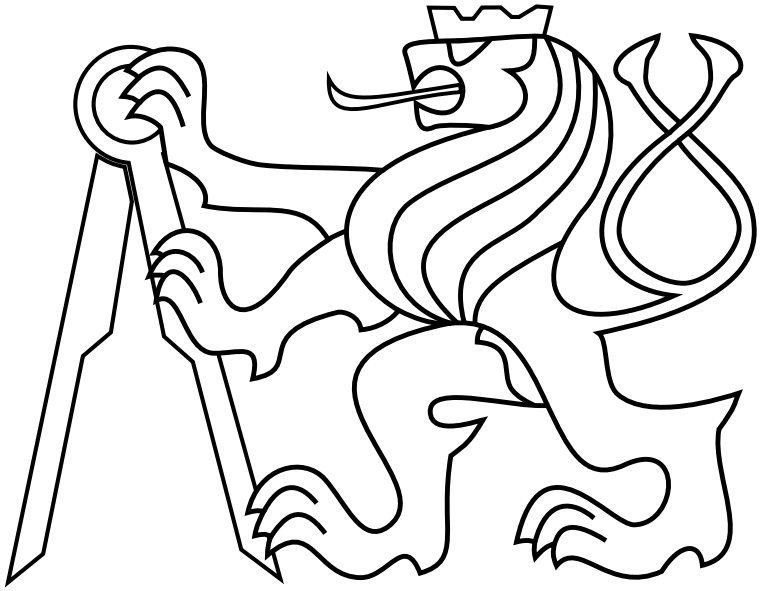

Ashwin Suresh Nedungadi

Design of an Electromagnetic Gripper for Unmanned Aerial Vehicles

Department of Cybernetics and Robotics

Thesis supervisor: **Dr. Martin Saska**

BACHELOR'S THESIS ASSIGNMENT

I. Personal and study details

Student's name: **Nedungadi Ashwin Suresh** Personal ID number: **464315**

Faculty / Institute: **Faculty of Electrical Engineering**

Department / Institute: **Department of Cybernetics**

Study program: **Electrical Engineering and Computer Science**

II. Bachelor's thesis details

Bachelor's thesis title in English:

Design of an electromagnetic gripper for unmanned aerial vehicles

Bachelor's thesis title in Czech:

Návrh elektromagnetického uchytovače pro bezpilotní helikoptéry

Guidelines:

The goal of the thesis is to design, implement and experimentally verify a magnetic gripper for construction of a wall by unmanned aerial vehicles (UAV). The task is motivated by the second challenge of the MBZIRC 2020 competition, https://www.mbzirc.com/challenge/2020.
1) Design the magnetic gripper and measure its performance with real test bricks for the MBZIRC Competition.
2) Design and experimentally verify a feedback system for the magnetic gripper using range finder and/or Hall sensors.
3) Develop and Integrate a feedback system, then estimate the feedback status through ROS into the system of Multi-Robot Systems group at CTU.
4) Testing and evaluation of the gripper in the laboratory and field testing with the complete system onboard the drone.

Bibliography / sources:

[1] V Spurny, T Baca, M Saska, R Penicka, T Krajnik, J Thomas, D Thakur, G Loianno and V Kumar. Cooperative Autonomous Search, Grasping and Delivering in a Treasure Hunt Scenario by a Team of UAVs. Accepted in Journal of Field Robotics, 2018.
[2] LaValle, S. M.. Planning Algorithms. Cambridge University Press, Cambridge, U.K., 2006.

Name and workplace of bachelor's thesis supervisor:

Ing. Martin Saska, Dr. rer. nat., Multi-robot Systems, FEE

Name and workplace of second bachelor's thesis supervisor or consultant:

Date of bachelor's thesis assignment: _____ Deadline for bachelor thesis submission: _____

Assignment valid until:
by the end of summer semester 2019/2020

Ing. Martin Saska, Dr. rer. nat.	doc. Ing. Tomáš Svoboda, Ph.D.	prof. Ing. Pavel Ripka, CSc.
Supervisor's signature	Head of department's signature	Dean's signature

III. Assignment receipt

The student acknowledges that the bachelor's thesis is an individual work. The student must produce his thesis without the assistance of others, with the exception of provided consultations. Within the bachelor's thesis, the author must state the names of consultants and include a list of references.

_____ .	_____
Date of assignment receipt	Student's signature

Declaration of Independent Work

I declare that the presented work was done independently and that I have listed all sources of information used within it in accordance with the methodical instructions for observing the ethical principles in the preparation of an university thesis.

In Prague on ....

Acknowledgements

I would like to thank my supervisor Dr. Martin Saska for his support and guidance during this project. I would also like to thank my advisor Ing. Daniel Heřt for his valuable inputs and for teaching me something about hardware. Furthermore, I would like to thank all the members of the Multi-Robot Systems group for their help with the outdoor experiments and for letting me be part of the team.
Finally, I would like to express my gratitude toward my parents who have shown incredible support, love, and encouragement during my studies.

Abstract

This thesis work deals with the design of a grasping mechanism for aerial grasping and assembly tasks by autonomous unmanned aerial vehicles (UAVs). The proposed design is aimed at solving ferromagnetic grasping by UAVs and has onboard sensors that detect and provide reliable feedback to the UAV. The main focus of the work deals with the design of the gripper, the technique used for feedback estimation and the integration of the entire mechanism into the current UAV systems at the MRS lab. Furthermore, an overview of the entire system and its implementation are discussed. The developed mechanism is tested multiple times under indoor and outdoor conditions and is designed to be deployed for Challenge II of the MBZIRC 2020 robotics competition in Abu Dhabi.

Keywords: unmanned aerial vehicle, aerial grasping, aerial object manipulation, sensor feedback

Contents

List of Figures

List of Tables

Chapter 1

Introduction

Contents

Unmanned aerial vehicles (UAVs) or Multi-Rotor Systems (Fig. 1.1) that are capable of vertical take-off and landing (VTOL) have undergone a revolutionary advancement in the past few years. They are being used for a wide range of applications in the consumer and technological sector from film making and photography, transportation [1][2][3] and autonomous delivery, hobby products and hobby flying to military applications [4][5] such as defense and reconnaissance systems. UAVs, with on board equipment are also ideal platforms for research [6][7][8] particularly in the areas of disaster relief, search and rescue as well as exploration [9][10] due to their low cost, small size and the variety of configurations in which they can be built.

These vehicles typically consist of 4 (quad-copters) or more rotors with fixed pitch propellers that are driven by brushless DC motors which together, produce thrust for the aircraft. By varying the thrust generated by the individual motors using ESCs (electronic speed controllers), the UAV can pitch, roll and yaw in a given direction.

With the improvement of hardware technologies and their growing applications, UAVs are being used in more complex tasks where interaction and manipulation with the environment are necessary, thus creating an increasing demand for the development of grasping mechanisms that can reliably lift, transport and manipulate objects.

Figure 1.1: Example of a UAV with onboard instruments, GPS antenna and battery

There are however, many challenges in such aerial grasping tasks as rotor aircraft are inherently susceptible to strong gusts of wind and disturbances during hover making the control of such UAVs a challenge. Other problems include limited payload capabilities of the UAV itself and flight stability with payload coupling as the attached payload changes the flight dynamics compared to free flight.
Moreover, the grasped object should be aligned with the center of mass of the UAV without which, the stability of the UAV is uncertain during transportation of the payload which may induce abnormal maneuvers or oscillations to the UAV, resulting in a crash.

The required grippers for such aerial tasks have to be robust mechanically and must be able to be controlled reliably by a pilot or the autonomous system onboard. They should also stay light-weight and draw the minimum power from the UAV's battery source to be used in practice.
For aerial grasping or autonomous transportation tasks, the designed gripper must be able to lift a variety of payloads and also be able to provide reliable feedback on the status of the said payload under outdoor conditions.
This thesis deals with the design and verification of a robust electromagnetic based grasping mechanism with a system for reliable feedback of the grasped object for autonomous aerial grasping and manipulation tasks for the upcoming MBZIRC 2020 robotics competition (Sec. 1.3.1).
The thesis work takes an iterative R&D approach, testing and refining various designs over multiple iterations. The design of the grasping mechanism, the approach used to estimate feedback using various sensors and the overall system is described in the following pages.

1.1 Problem statement

The primary objective of this thesis is to design and experimentally verify an electromagnetic grasping mechanism with suitable feedback to be used in an assembly task by a group of UAVs using a range of bricks with different masses and sizes and deploy it for the second challenge of the MBZIRC 2020 competition.
The designed gripper system is then integrated within the UAV system with control and feedback in ROS (Robot operating system). Furthermore, we provide an overall description of the current systems in development for the MBZIRC 2020 competition along with the analysis of the data from the designed gripper during different outdoor experimental tests.

1.2 Structure of this thesis and contribution

This thesis work is structured into 6 main chapters as follows:

- The first chapter gives an introduction to the problem, the challenge and source of inspiration and also discusses related works in detail. Most of the cited research works focus on the topics related to the theme of this thesis.
- In the second chapter we establish some preliminary conditions and discuss various principles necessary to fully understand the problem and solution design.
- In chapters 3 and 4, we provide the description and design of the proposed grasping mechanism, the algorithms and also include certain high level and low level aspects of the system.
- In chapter 5 we present the description of the overall UAV system as well as experimental data from test flights followed by some analysis and discussion of the experiments, and in chapter 6 finally we conclude the work.

This thesis contributes directly to the research done for the MBZIRC project where we present [11] a novel idea for an electromagnetic grasping mechanism that can lift theoretical payloads of up-to 6 kg. The designed gripper is robust and can lift a range of ferromagnetic payloads from small loads of 100 g to 6 kg. The designed gripper is thoroughly tested in multiple outdoor experiments and through iterative design refined into a final prototype to be used for the competition.

1.3 MBZIRC competition

The Mohamed Bin Zayed International Robotics Challenge (MBZIRC) [12] is an international robotics competition that is held every two years in Abu Dhabi, United Arab Emirates and comprises of various demanding challenges in which the best university teams in the world compete in attempts to solve the challenges (Fig. 1.2) for maximum amount of points.

The objective of the MBZIRC competition is to provide an ambitious and technologically demanding set of challenges in robotics intended to demonstrate the current state of the art in robotics in terms of scientific and technological accomplishments, and to inspire the future of robotics.

In the MBZIRC 2017 competition, the team led by Multi-Robot Systems group from Czech Technical University won various prizes in the different challenges presented. The team comprised of 20 members as a part of a larger collaboration effort between the University of Pennsylvania, University of Lincoln.
The most notable and relevant prize won by the team to this thesis was the first place in the third challenge where a group of 3 UAVs had to locate and retrieve circular metallic disks and drop them in a defined drop zone in a "Treasure Hunt" scenario. This thesis builds upon the lessons learnt from the MBZIRC 2017 experience and contributes towards the upcoming MBZRIC 2020 competition.

Figure 1.2: A UAV attempts to grasp a dynamically moving item on top of a turtle bot while another UAV transports the already grasped item to the drop zone (MBZRIC 2017)

1.3.1 MBZIRC 2020

The next MBZIRC competition is scheduled for February of 2020 in Abu Dhabi with over 30 international teams competing for the prizes. MBZIRC 2020 will be based on autonomous aerial and ground robots, carrying out navigation and manipulation tasks under harsh indoor and outdoor conditions.
MBZIRC 2020 will consist of three individual challenges and a triathlon type Grand Challenge which is a combination of the first three challenges. The challenges will be focused in the areas of UAV tracking & interaction, construction automation and urban fire-fighting:

- In challenge I, the first task requires a team of UAVs to autonomously detect, track and eliminate a set of balloons in an open field, the second task requires a UAV to chase and catch a ball that is being transported by another UAV. Challenge I is motivated by precise detection and elimination tasks by UAVs and UAV safety.
- In challenge II, a team of 3 UAVs along with a UGV (unmanned ground vehicle) detect, grasp, transport and assemble different types of bricks into a pre-defined structure in an outdoor environment. This challenge is motivated by autonomous construction using robots.
- In challenge III, the same team comprising of 3 UAVs and a UGV is required to work cooperatively to extinguish a series of simulated fires in a building structure under an urban fire-fighting scenario.
- In the final Grand Challenge, the team of autonomous robots work together to attempt to solve all the 3 challenges simultaneously in a timed event.

1.4 State of the art

There are several available solutions for aerial grasping. Many of which focus on passive magnetic grasping and robotic claw like manipulators for the grasping or aerial manipulation of objects. We will discuss each of the various techniques proposed and their advantages and disadvantages for aerial grasping tasks.

One such example of a solution for aerial grasping includes work done by the RISC laboratory at King Abdullah university of science and technology [13] where a passive magnetic gripper with an impulse release mechanism and push-button feedback was developed. The design uses 16 small neodymium magnets which together produce the required magnetic force to grasp a ferromagnetic object. The release of the grasped object is facilitated by two high speed servos which pushes the drop plate and produces a high impulse release of the object.
While this kind of grasping mechanism provides a low-power passive solution, the grasping

capabilities provided by permanent magnets are inferior compared to that of an electromagnet in terms of magnetic strength and control. Furthermore, the release mechanism that relies on servomotors to separate the grasped object with impulse is bulky and adds another layer of unnecessary complexity to the system.
A scaled up version of this concept was also developed by the KAIST team [14] for MBZIRC 2017 competition. The system integrated contact sensors and 2 camera modules on the gripper for visual servoing and used 13 neodymium magnets and 4 servomotors that actuated the drop plate to forcefully separate the grasped object from the gripper.

Another popular solution for magnetic grasping utilizes electro-permanant magnets (EPMs) due to their low-power consumption (table 3.1), payload capabilities and ability to toggle the magnetic strength by magnetizing and demagnetizing the EPM with the help of an active external switching circuit.
This solution was used by several teams, including our own team in the 2017 MBZRIC competition using the COTS[1] OpenGrab EPM V3 from nicadrone [15][16][17].
A custom EPM based solution was also presented in the work [18] by ETH Zurich which has the ability to grasp ferromagnetic objects with a curvature of up to 30 degrees and utilizes alnico and neodymium magnets. Another custom solution was tested in the MRS lab for cooperative grasping by UAVs in the master's thesis work [19] which used servomotors to rotate neodymium magnets by 90 degrees for grasp and release.
Although electro-permanent solutions are popular candidates for aerial grasping and manipulation tasks and offer low-power solutions, they come with many disadvantages. They are expensive, do not scale well with mass, have low payload capabilities and require an active control circuit to magnetize and demagnetize the magnet. Furthermore, there is a need for firm contact with the ferrous surface in order to grasp the object successfully.
Moreover, as experienced by our team [16] and other teams [15][17] during the last MBZIRC 2017 competition, the magnet can also break if used with heavy force and the circuitry can burn out if the command signal is sent multiple times resulting in many gripper failures and an overall low success rate [17]. The teams also found that the EPM solution provided to be too weak in outdoor conditions where gripper failure was even caused due to the thick layer of paint on the objects in the competition [15][16][17].

There exists several unique ideas for aerial grasping developed over the years such as impactive or claw based, ingressive grasping techniques and suction based grasping.
Impactive grasping mechanisms that are modeled after claws or human arms are widely studied problems in robotics. They are also used by industrial robots as end effectors for various automation tasks. Over the years there have been several publications regarding these mechanisms[20][21][22] each optimized for a specific task with it's own set of advantages and disadvantages. Although such mechanisms offer a robust solution to grasp a wide range of objects with different shapes, they are far too complex and heavy to be used onboard UAVs. However, there are many existing simplified grasping mechanisms [23][21]

[1] Commercial off-the-shelf

and they have been proven to be suitable for grasping of wooden blocks and packages. But considering the requirements for the MBZIRC 2020 competition and the engineering complexity of developing such a mechanism, we had to eliminate such grasping techniques. Moreover, under a competitive scenario it is crucial that the hardware engineers are able to quickly debug and resolve any issues that could arise and having a complex system onboard multiple UAVs would be more of a liability to our team than a strength.

Two unique solutions for aerial grasping are presented in the works [24][25]. The first being a self-healing suction mechanism that utilizes an onboard vacuum pump that produces the sufficient volume flow to grasp a variety of payloads. Although the possibility of using suction for aerial grasping proves to be a great solution for non-magnetic object grasping and grasping of items with small curvature, the disadvantage of having a big enough compressor for heavy payloads and sufficient volume flow onboard the UAV combined with its complexity made it a clearly unsuitable candidate for our task.
The other grasping mechanism for aerial grasping utilizes an ingressive gripper. The mechanism consists of metallic "claws" or "hooks" driven by servo motors which penetrate the surface of the object to be grasped and hooks itself into the surface, allowing the UAV to carry the object. The hooks are then retracted using the servo motors when the UAV needs to release the object.
Such a mechanism is very useful as demonstrated in the work [25], to transport wooden blocks or packages with strong cardboard linings. However, it is impractical when it comes to rigid or delicate objects as it relies on penetrating the surface to grasp and makes an indent in the process which in the long term proves to be impractical and especially unsuitable for our task as the objects we want to grasp will be metal.

While the above mentioned aerial grasping solutions are not as simple or heavy payload compatible, our solution is designed for ferrous payloads and provides reliable feedback using multiple sensors on whether an object is successfully grasped or not. Moreover, electromagnets provide the solid advantage of scalability to the system while being cheap and can be hot swapped on the field to accommodate heavier or lighter payloads or in case of failure. The mechanical design of our gripper is developed with reliability and operation in outdoor desert conditions in mind while being able to lift ferrous objects weighing theoretically up to 6 kg with the only limitation being the payload capacity of the UAV used.

Chapter 2

Preliminaries

Contents

In order to proceed with the rest of the thesis work, we need to establish some knowledge of the working principles involved. This chapter gives a brief introduction to the physical concepts and theory involved.

2.1 Robot Operating System (ROS)

ROS [26] is an open-source, meta operating-system running on Unix-based platforms and is widely used by the robotics community.

It provides the services expected from an operating system, including hardware abstraction, low-level device control, implementation of commonly-used functionality, message-passing between processes, and package management. It also provides various tools and libraries for obtaining, building, writing, and running code across multiple computers.
The basis of ROS is made up of packages, where all the software are located in the form of executable and supporting files.

A node in ROS is a process that performs some computation. Nodes in ROS can receive or publish messages known as “topics” to other nodes in a distributed manner. A robotic

system usually comprises of many nodes each of which does a specific task. For example, one node controls a laser range-finder, one node controls the thrust inputs to a controller, one node performs path planning, one node publishes diagnostics about a running process, and so on. Nodes can also call upon other nodes to do a specific task in the form of ROS services. ROS services are bi-directional messages and expect a reply from the receiving end.

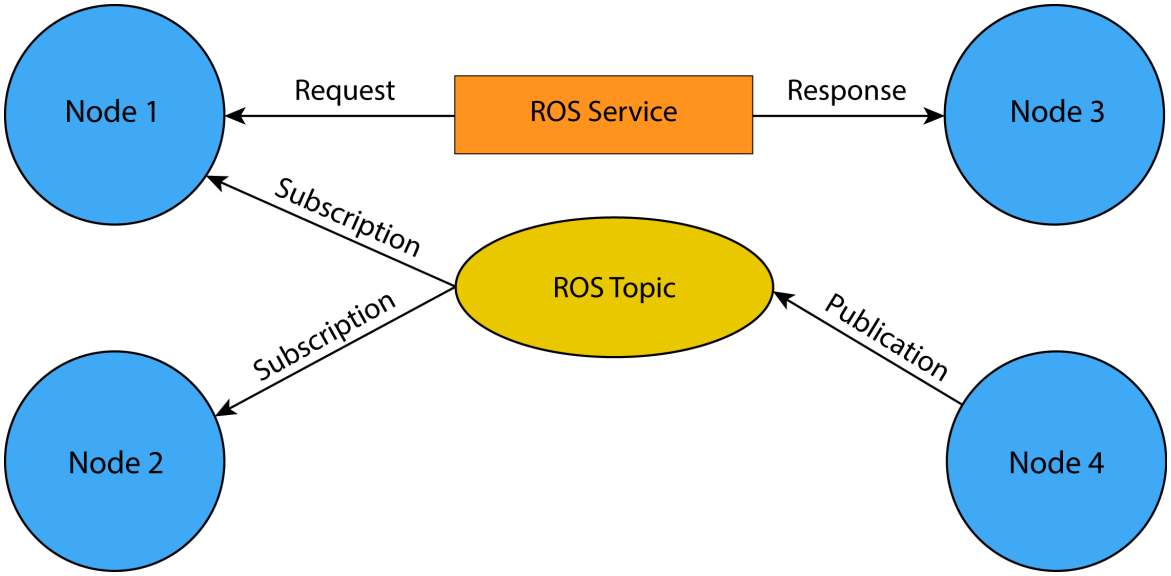

Figure 2.1: Diagram of how communication between nodes work in ROS

A ROS distribution is a versioned set of ROS packages. These are akin to Linux distributions (e.g. Ubuntu). The purpose of the ROS distributions is to let developers work against a relatively stable codebase until they are ready to roll everything forward.
Various distributions of ROS are used in the robotics community, the latest being Lunar Loggerhead. We however use Melodic Morenia for the purpose of our tasks.

2.2 Concepts of Electromagnetism

An electromagnet is a device consisting of a core of soft magnetic material[1] surrounded by a coil through which an electric current is passed to magnetize the core. By definition, this means that an electromagnet can be turned on and off by passing current through it's coil making it highly suitable for a wide range of applications.

Engineering an electromagnet is systematized by known equations that characterize a magnetic circuit and which decide certain properties of the designed electromagnet such

[1]Soft magnetic materials are those materials that are easily magnetised and demagnetised. They do not retain their magnetism after the electric current is removed.

as holding force.
The holding force of an electromagnet is defined as the force which is perpendicular to the attraction surface of the holding magnet.
The force exerted by a magnetic field or the holding force of an electromagnet is described by the equation:

$$F_h = \frac{B^2 A}{2\mu_o}, \tag{2.1}$$

for a closed magnetic circuit with no air gap:

$$B = \frac{NI\mu}{L}. \tag{2.2}$$

Where B is the magnetic flux density; A is the cross sectional area of the core; N is the number of turns of coil winding; I the current in the winding coil and L, the length of the magnetic field path.
The constants μ and μ_o being the permeability of the electromagnet core material and permeability of free space respectively.

Substituting (Eq. 2.2) into (Eq. 2.1), we get the relationship for the holding force of an electromagnet:

$$F_h = \frac{N^2 I^2 \mu^2 A}{2\mu_o L^2}. \tag{2.3}$$

Electromagnets are also subject to side effects, some of which that must be discussed here as they will become relevant later [27][28][29].

1. **Power losses due to Ohmic heating**: In electromagnets, it is common for energy to dissipate as heat due to the resistance of the windings which scales proportionally as the size of the electromagnet begins to increase.
   Electromagnets come in various thermal insulation classes, which is categorized by a limiting temperature beyond which the performance of the electromagnet will be affected[2].
   The ohmic heating effect can be reduced by limiting the current in the coils or using thicker coils to decrease their resistance.

2. **Inductive voltage spikes during disconnection**: Electromagnets have significant inductance which resists changes in the current through its windings, sudden changes in the winding current causes large voltage spikes across the windings.
   This is because when the current through the magnet is increased, such as when it is turned on, energy from the circuit is stored in the magnetic field. When it is turned off the energy in the field is returned to the circuit. Thus, when an electromagnet is disconnected, the energy in the magnetic field is suddenly returned to the circuit, causing a large voltage spike and an arc across the switch contacts. The electrical

[2]The magnet used in this project has an insulation class of B (130^0 C)

circuits involving electromagnets usually counter this problem with the help of a "freewheeling diode" or "fly back diode" [30] connected across the electromagnet. Large electromagnets avoid this by using power circuits controlled by a microprocessor that achieves current changes slowly, in gentle ramps taking several minutes to energize or deenergize the magnet.

3. **Remanence effect**: Remanence or residual magnetic field [31][32] is the magnetization left behind in a ferromagnetic material after the external magnetizing field is removed. This effect is known to occur in electromagnets causing the payload to be attached to it even after the electromagnet has been turned off. This problem can be countered by a process known as degaussing or in our case, a quick polarity change of the electromagnet voltage.

4. **Variation of holding force as a function of surface thickness**: From our earlier equation (Eq. 2.1), the holding force of a magnet is characterized by the square of it's flux density [33]. Hence, the holding force of an electromagnet relies on the thickness of the part to be held.
The thicker the target surface is, the greater the number of magnetic field lines passing through the object (Fig. 2.2 from [28]). Therefore, if the part to be held is too thin then it will not be able to accommodate all the available field lines and will become saturated. The force will then be inadequate and the electromagnet will be unable to hold on to such a thin surface.

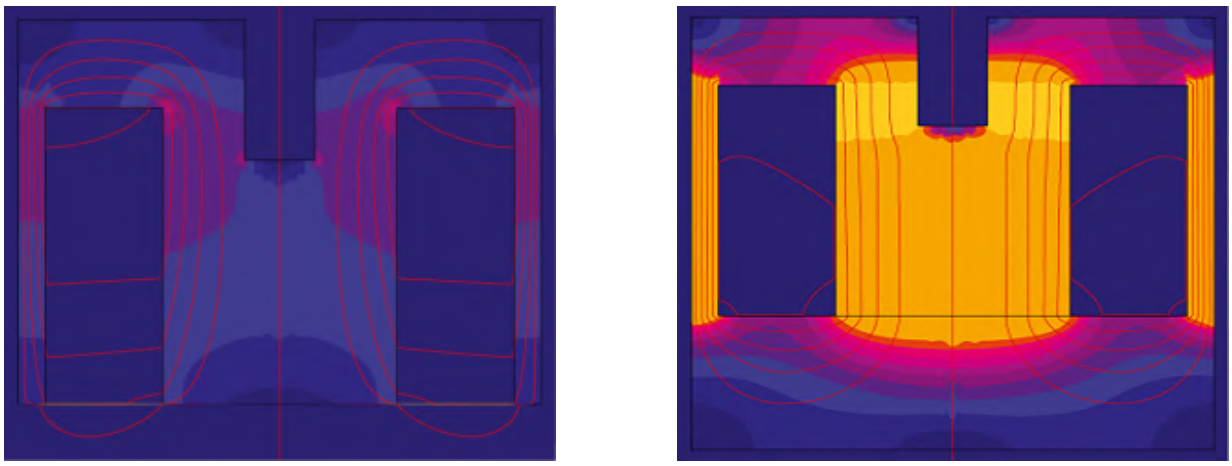

(a) Surface of thickness 0.2 mm

(b) Surface of thickness 10 mm

Figure 2.2: The variation of magnetic field and flux with thickness of surface

2.3 Sensors used and working principles

A few different types of sensors were considered for the feedback of whether a brick was successfully grasped or not as this was a critical task for autonomous grasping. We will look into the principles of their working.

Distance Sensing with Ultrasonic Sensor

Ultrasonic sensors work by emitting sound waves at a high frequency then wait for the sound to be reflected back, calculating distance based on the total time (Fig. 2.3 from [34]). This is similar to how radar measures the time it takes a radio wave to return after hitting an object. For this reason an ultrasonic sensor has an ultrasonic emitter and receiver.
We know the elementary formula $Distance = Speed * Time$, thus by measuring the time taken by an ultrasonic wave to be reflected off an object and detected up the sensor again, we can formulate:

$$d = c.\frac{1}{2}\ t \tag{2.4}$$

where d is distance and is given by the product of c - speed of sound in air at room temperature ($\approx$ 343 m/s) and t - the total transmission time.

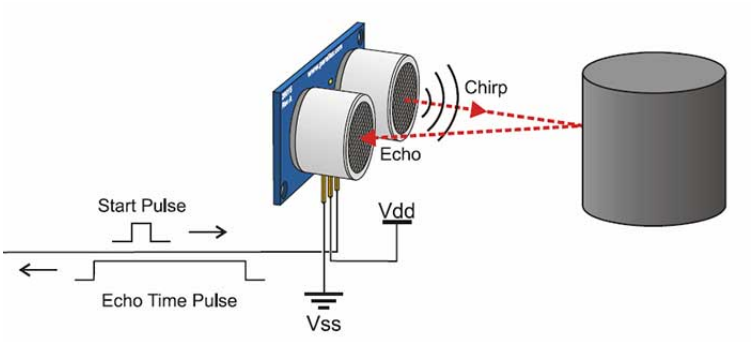

Figure 2.3: Working principle of an ultrasonic sensor

Distance Sensing with Inductive Proximity Sensor

Inductive proximity sensors are non-contact measurement devices used in detection of metallic objects. Their operating principle is based on a coil and oscillator that creates an oscillating electromagnetic field in the close surroundings of the sensing surface (Fig. 2.4 from [35]). The presence of a metallic object in the operating area causes a dampening of the oscillation amplitude due to energy loss by induced eddy currents in the metallic object.
The rise or fall of such oscillation is identified by a threshold circuit that changes the output of the sensor. In the sensor used for this thesis[3], this threshold was at 2 mm distance from the sensor.

[3]The sensor used is the LJ8A3-2-Z Inductive Proximity Sensor with sensing capability of upto 2 mm.

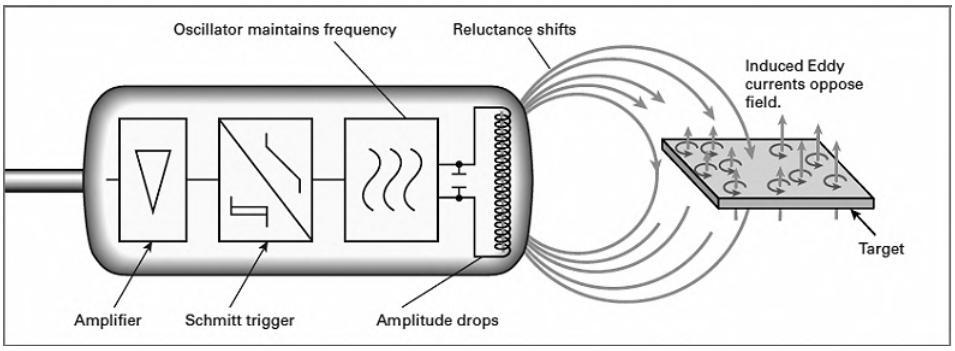

Figure 2.4: Working principle of an inductive proximity sensor

Magnetic Sensing with Hall-Effect Sensor

A Hall effect sensor is a device that is used to measure the magnitude of a magnetic field (Fig. 2.5 from [36]). Its output voltage is directly proportional to the magnetic field strength through it.
Hall effect[4] sensors are used in various areas to measure position, speed, and magnetic field. The principle of semiconductor hall sensors is that when a current-carrying semiconductor is introduced to a magnetic field, the charge carriers of the semiconductor experience a force in a direction perpendicular to both the magnetic field and the current[5] and hence a voltage appears at the semiconductor edges.

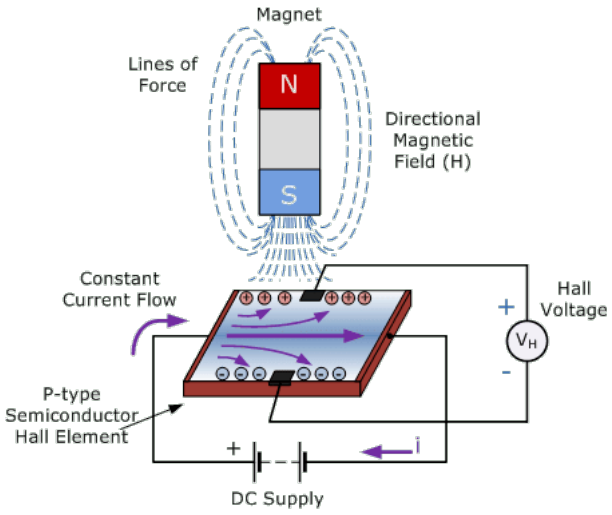

Figure 2.5: Working principle of a hall-effect sensor

[4]The sensor used is a linear hall effect sensor SS49e
[5]As per Fleming's right hand rule

2.4 Forces acting on a UAV with coupled payload

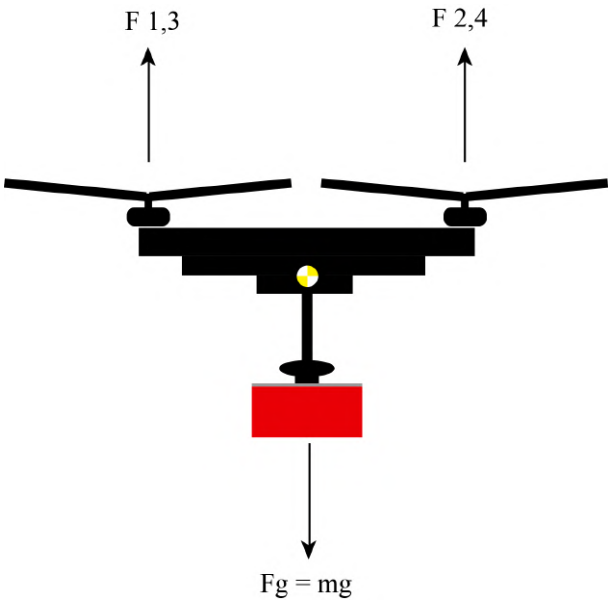

Figure 2.6: Free body diagram of UAV with coupled payload

The forces acting on the UAV [37] behaves differently based on if a payload is attached rigidly or can move about some axes. In the case of rigid mechanics, There is a force acting downward (Fig. 2.6) $\vec{F_g} = m\vec{g}$ which needs to be compensated by the collective thrust produced by the UAV $\vec{F_c} = \vec{F_1} + \vec{F_2} + \vec{F_3} + \vec{F_4}$. The thrust force $\vec{F_i}$ of a rotor can be given by the formula:

$$\vec{F_i} = K_f \ \omega^2 \tag{2.5}$$

Where ω is the rate of rotation of the propellers and K_f is a proportionality constant that depends upon many factors like torque proportionality constant, back-EMF, Density of surrounding air, area swept by propeller etc. and is measured empirically.
At equilibrium (hover condition), the collective thrust generated by a quadrotor balances out the weight of the drone as:

$$\sum_{i=1}^{4} K_f \ {\omega_i}^2 + m\vec{g} = 0 \tag{2.6}$$

But suppose the thrust is more than the mass, in this case the quadrotor accelerates upward and the equation is given by:

$$\sum_{i=1}^{4} K_f \ {\omega_i}^2 + m\vec{g} = m\vec{a} \tag{2.7}$$

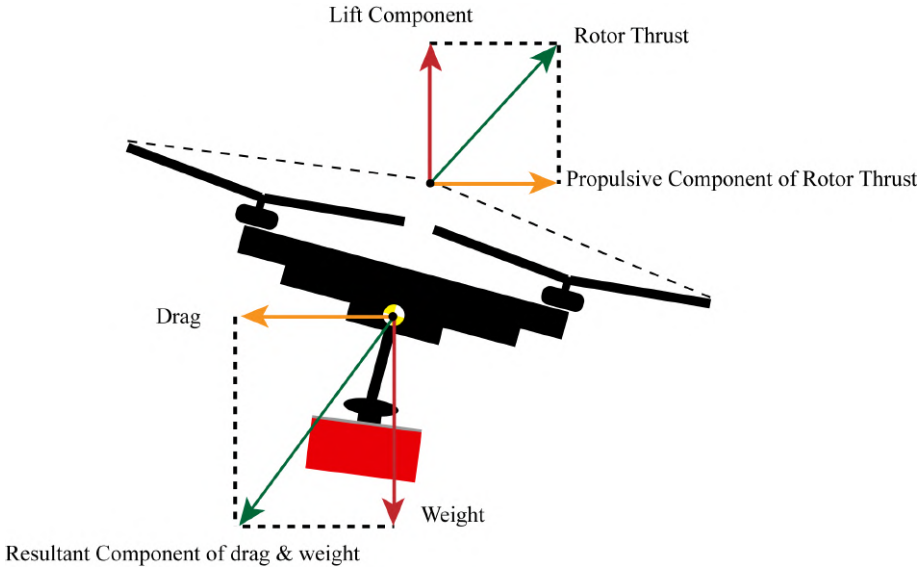

Figure 2.7: Forces acting on a UAV in forward flight

A UAV in flight, is acted upon by four basic aerodynamic (Fig. 2.7) forces [38]:

1. **Lift**: Lift is the force that opposes the downward force of weight and is produced as a result of the motion of the propellers through air [39]. It depends on factors such as speed of airflow, density of air, area and pitch of the used propellers. For a quad-copter, the maximum lift produced is fixed due to the fixed pitch propellers and maximum rpm (revolutions per minute) generated by each motor.

2. **Weight**: Weight is the combined load of the UAV itself, including the instruments, air-frame, payload and battery. It pulls the UAV downward due to the force of gravity and opposes lift vertically in the opposite direction through the center of gravity. In most cases, the weight of the UAV is fixed and known.

3. **Thrust**: The force produced by the rotors is called thrust. It can be forward, rearward, sideways or vertical. The UAV attitude and thrust determines the direction of movement of the UAV.

4. **Drag**: The drag force is a rearward, retarding force caused by wind resistance and disruption of airflow by the rotor, air-frame and payload. It opposes thrust.

In the case of a coupled payload, a certain degree of freedom can complement the UAV's ability to carry and transport the payload while reducing mechanical stress and strains on the grasping or suspension mechanism. However, a new problem arises where the disturbances during flight cause the coupled payload to swing around like a pendulum. This problem is widely studied [40][41] but cannot be easily overcome in the real world without the proper position and orientation feedback of the payload and the aerodynamic interactions due to the downward airflow from the UAV.

2.5 Parameters of tested bricks

To simulate the correct conditions for our outdoor experiments, it was necessary to manufacture and test our systems on the proposed bricks from the MBZRIC 2020 organizers. A complete list of the challenge criteria and parameters of the objects involved can be found online [12].
The manufactured test bricks used Styrofoam, adhesive and metal sheets of various thickness providing the necessary mass for the proposed bricks[6]. Multiple bricks were manufactured with the heaviest variant being 4 kg (blue) and the lightest being 0.75 kg (red). The tested bricks and their parameters are shown in table 2.1.

Brick Color	**Dimensions**	**Mass**
Red	0.30 m x 0.20 m x 0.20 m	0.75 kg - 1.0 kg
Green	0.60 m x 0.20 m x 0.20 m	1.40 kg - 2.0 kg
Blue	1.20 m x 0.20 m x 0.20 m	2.36 kg - 4.0 kg

Table 2.1: Parameters of tested bricks

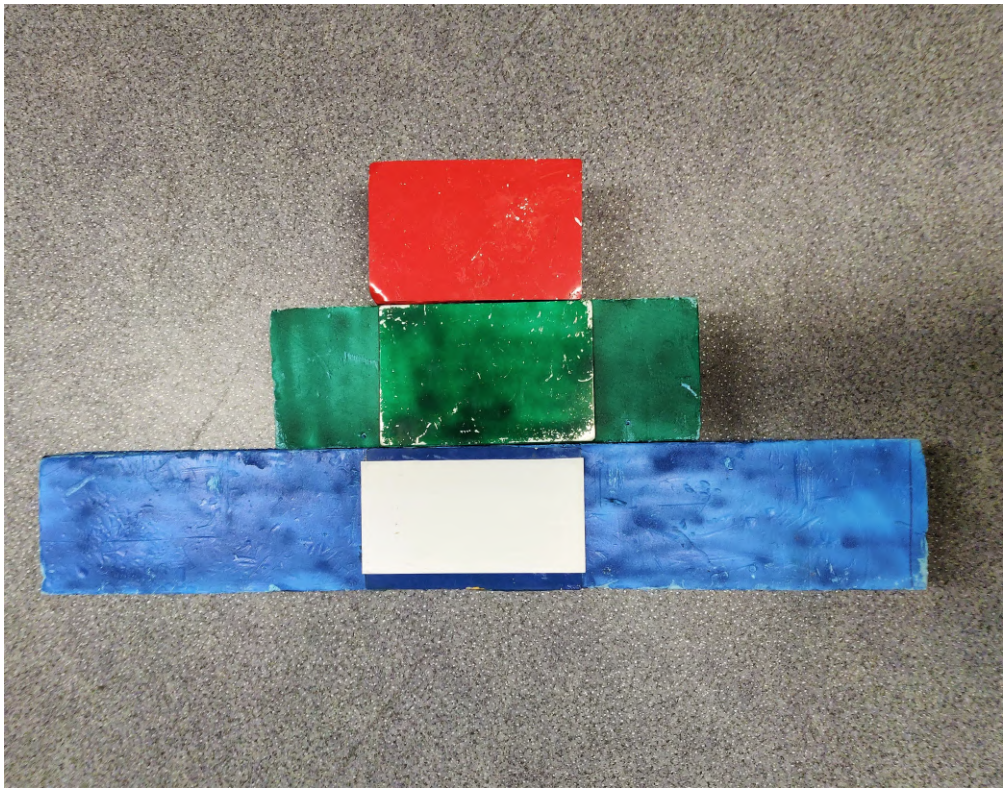

Figure 2.8: Manufactured test bricks

[6]The manufactured bricks were made to be worst case scenarios of the described parameters from MBZIRC 2020, hence they exceeded the competition requirements.

Chapter 3

Description of the Gripper

Contents

Aerial grasping and manipulation is a well known problem in the field of modern aerial robotics. They are also highly desirable capabilities that an unmanned aerial vehicle can possess.
In most cases however, commercial based aerial grasping mechanisms such as magnetic or suction-based end effectors designed for industrial robots, are not suitable for autonomous aerial operation or robust enough to be employed so. Therefore, custom designed grasping mechanisms are often favored because the current state of the art in 3D printing technology makes it accessible to rapidly prototype such custom solutions and the fact that they can be customized for specific applications and adapted on the field makes it an ideal choice for research and development.

The designed grippers for aerial manipulation and transportation tasks must be engineered to be mechanically robust and compliant while considering the following requirements:

- Lightweight
- Sufficient holding force for payload
- Low power consumption
- Autonomous control and reliable feedback

- Fail-safe grasp and release

A viable aerial grasping mechanism will have to fullfill the above conditions to be used onboard an autonomous UAV in outdoor conditions.

3.1 Tested Iterations

Following the methodology for iterative designing, we have tested multiple prototypes for a suitable electromagnetic grasping mechanism while rejecting bad designs and reinforcing promising ones through trial and error.

EPM based solution

The gripper (Fig. 3.1) used for MBZIRC 2017 [16] consisted of an Electro-Permanent Magnet (EPM) end effector attached to a ball joint that could freely rotate in all directions and a compression spring along the shaft that connects it to the UAV.
Although this worked well for the task described by the competition (Sec. 1.3), several groups who participated (Sec. 1.4) experienced problems with the EPM based solution [15][17] including our team from CTU.

The primary problem was the burning of the control circuit on the OpenGrab V3 EPM when the command signal for activation is sent multiple times as this was done to strengthen the holding force after an object was initially grasped. Secondly, the EPM is very delicate for outdoor environments as dirt or gravel could be crushed into the surface causing an insulation breakdown [42]. Furthermore, it provided to be weak in terms of holding force as it only had 15 kg of holding force which was effectively reduced it to 2.25 kg in shear [16] and even lower considering the forces acting on it during flight [38].

Another problem encountered by our team was due to the design of the mechanical ball joint which had unlimited freedom in the yaw axis, which meant that any object grasped in flight would yaw along the directions of the acting forces and considering that the competition took place near the sea and was affected by strong sea breezes, this became problematic.
Since the next competition requires UAVs to transport long cuboidal bricks, a ball joint would be highly undesirable due to the uncontrollable yawing motion caused by the different forces on the payload in flight [38].
Considering all the above problems it was decided to abandon any EPM based solution for the next MBZIRC as the objects described were bigger and have masses upward of 1 kg.

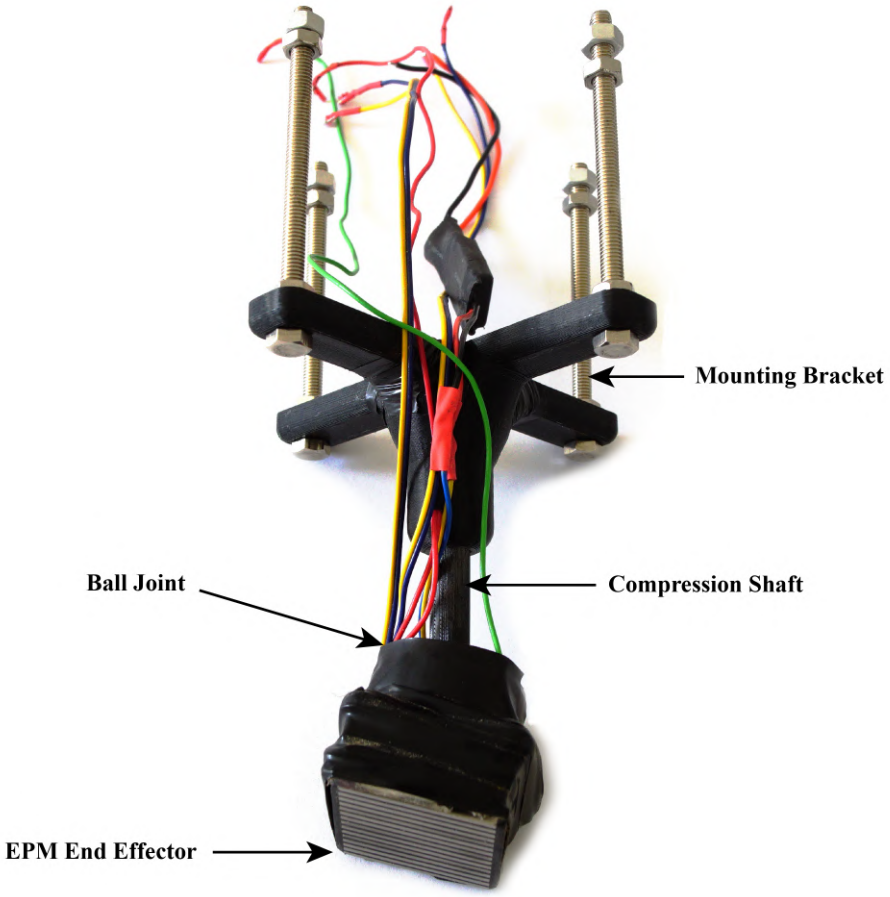

Figure 3.1: Gripper used for MBZRIC 2017

Dual electromagnets with ultrasonic-hall feedback

While going through the design process for the gripper, it was crucial to come up with a design that was capable of grasping and transporting the proposed long brick-like objects in challenge II (Sec. 1.3.1).
Our hold force and power requirements were satisfied by a single electromagnet which had dimensions of 49/21 mm and was capable of lifting up to 40 kg under ideal conditions.
The problem then is to take into consideration that the longest brick to be grasped was 1.2 m long and weighed 1.5 kg. For such a long brick, the placement of two electromagnets of lifting power 40 kg each separated by a distance of 20 cm was ideal[1] as the gripper would experience fewer torque effects (Fig. 3.3). As the challenge is timed, it is important to transport the bricks as fast as possible without causing disturbances to the payload or UAV. Hence, by grasping the brick at 2 positions, the drone could fly faster safely. The

[1]The separating distance of 20 cm was chosen as it was the right distance to accommodate even the smallest brick which was 0.3 m long

gripper was attached to the UAV with the help of a mount which facilitated movement along the roll and pitch axes and not in the yaw.

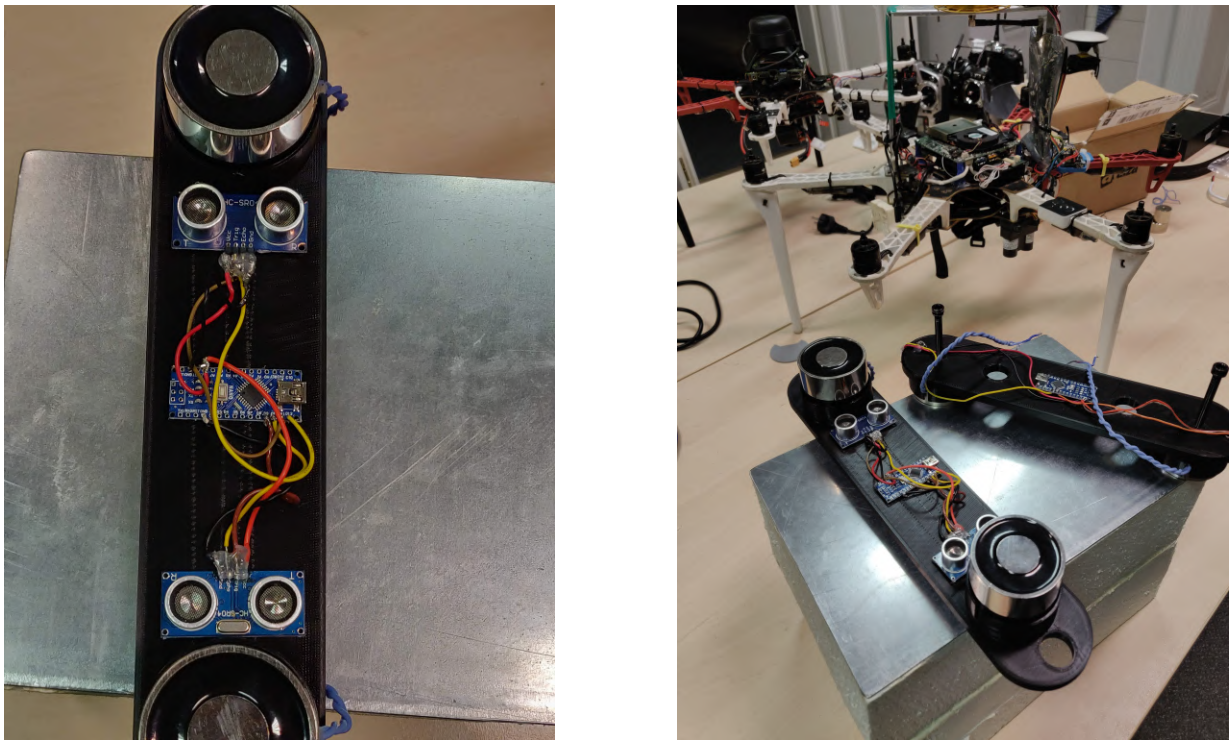

Figure 3.2: Gripper prototype with ultrasonic sensors and onboard MCU

Figure 3.3: The dual-grasping gripper during test flight

During the preliminary tests (Fig. 3.4), three prototypes of the gripper were tested, one with dual ultrasonic feedback (Fig. 3.2); the second with feedback from hall effect sensors: and finally a prototype that combined the ultrasonic sensors with proximity sensors to calculate total feedback of the gripper. The signal processing for feedback from each prototype is discussed in the next chapter.

Although by the design of the 2-DOF mount, the mechanism was able to align the grasped brick to the center of gravity (Fig. 3.3), there was a major drawback with the prototype. The long design of the dual grasping mechanism meant extra unnecessary weight, redundant sensors and twice the power consumption by the two electromagnets which translated to limited operating time before the batteries had to be changed. Moreover, due to the longer design, the gripper exhibited unstable "see-saw" like motion during flight when there was no payload due to the slight variation of forces acting on either ends due to downwash generated by the propellers and wind.
Due to the above reasons and due to the fact that there was a clear trade-off between the electromagnet's hold force and power consumption, there was a need to simplify and miniaturize the design.

(a) The UAV in flight without payload

(b) Gripper with partial grasping of brick

(c) UAV in front of wall structure

(d) UAV attempts to place a brick

Figure 3.4: Experimental manual flights with onboard gripper prototype

Rigid Gripper

Another prototype proposed and tested by the MRS Lab was the idea of a solid gripper with a linear array of electromagnets that can grasp the brick horizontally. This prototype consisted of two smaller electromagnets of 25 kg holding force each and had hall sensors embedded on their surfaces for feedback. The base would attach via a solid compression shaft that is completely rigid and 3D printed as shown in Fig. 3.5.

While the solid design offers good brick placement for building a wall, such a design is not very robust as the forces during flight will act on the payload coupled UAV and cause high drag and mechanical strain on the gripper itself as well as decrease the hold force of the magnets [16]. To compensate for this, the UAV's maneuvers and speed have to be severely restricted so that the brick does not fall down during transportation. Moreover, high quality of the 3D print has to be ensured without which, the base would fracture from the shear forces of flight.

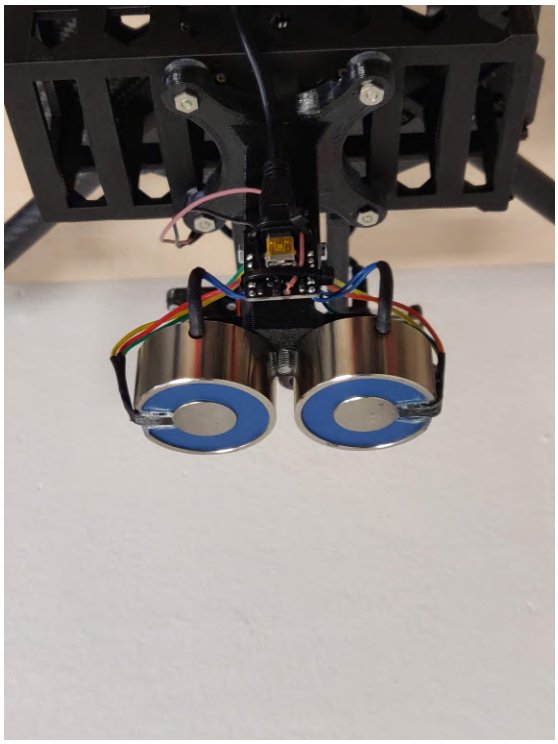

(a) Side view showing the MCU, the compression shaft and mounting for the UAV

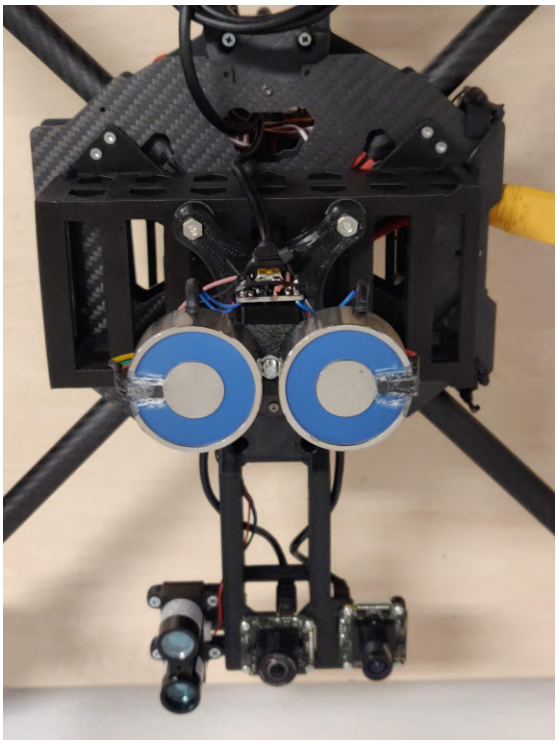

(b) Bottom view showing the embedded hall sensors on the electromagnet surface

Figure 3.5: Prototype of the rigid gripper with embedded hall-sensors and MCU

3.2 Proposed gripper design

The current proposed design of the gripper consists of 4 major components:

1. An electromagnet with switching circuit
2. Gripper housing with compression shaft and mounting attachment
3. A combination of a hall-effect sensor embedded in the electromagnet and inductive proximity sensor for feedback
4. Arduino MCU that processes raw signals from the sensors, communicates with the on-board computer and also controls the switching circuit of the gripper.

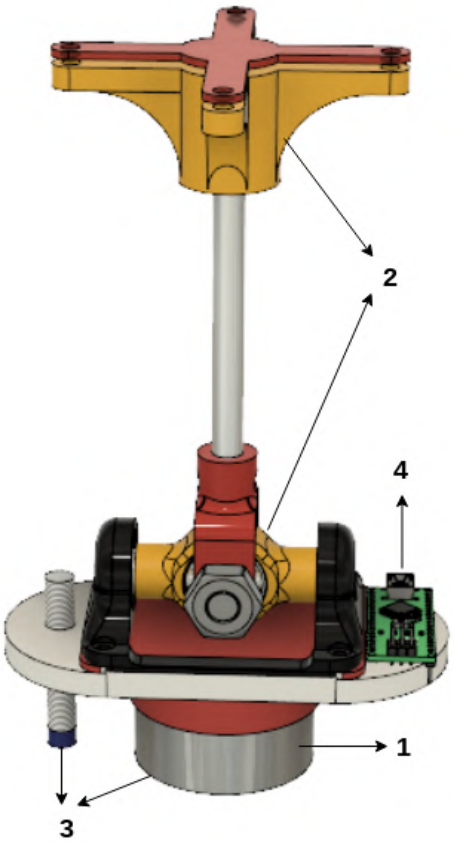

Figure 3.6: Modeled CAD assembly of proposed gripper showing 1. Electromagnet, 2. Gripper housing, 3. Sensors used for feedback, 4. Arduino MCU

Electromagnet and switching circuit

An industrial electromagnet capable of lifting up-to 40 kg of payload provides the necessary magnetic hold force for grasping. The electromagnet is supplied a constant 12 V DC for its operation and has a custom built N-MOSFET switching circuit integrated with the Arduino that can be toggled by the UAV's onboard computer (Sec. 2.1). Although the electromagnet consumes 10 W, it is insignificant compared to the power drawn by the UAV's onboard computer (60 W) and motors (1000 W) from the 8000 mAh (178 Wh) Li-Po Battery. And considering the magnets won't be turned on and in operation continuously throughout the flight, there is no particular reason to be concerned by the electromagnet's power consumption.

Gripper housing and mount

The gripper base (Fig. 3.7a) and mounting bracket is designed to be sturdy structurally and is fabricated using 3D printing technology with PLA and ABS plastic.
It has 2 degrees of freedom in the pitch and roll axes and consists of a main mount where the sensors, magnet and MCU are fixed, an inner and outer ring structure with ball bearings (Fig. 3.7c) to facilitate the movement along the two described axes and a shaft with a mounting bracket so it can be attached to the UAV with 4 screws and nuts (Fig. 3.7b) (Fig. 3.7d). By the mechanical design of the gripper, the angle of rotation for the 2 axes are restricted to approximately 30 degrees, this ensures that the grasped object does not swing too much and cause a disturbance for the drone.

Feedback sensors and signal processing

Reliably estimating the status of a successful grasp is a crucial task for aerial autonomous grasping. The gripper integrates feedback from two independent sensors: A hall sensor embedded in the electromagnet's surface and an inductive proximity sensor mounted on the side. The raw analog signal is first digitized by the Arduino's 10-bit ADC (analog-digital converter) and is then processed using an algorithm and a final feedback is given using a combination of the feedback from the individual sensors.

The chosen MCU for prototyping the gripper is an Arduino nano as it is low-power (≈ 0.1 W), open-source and easy to program in the Arduino IDE. It also has 8 analog pins with a 10-Bit ADC for acquiring signals as well as 22 digital I/O pins which makes it very convenient to use in rapid prototyping.
The electronic components of the gripper consist of the electromagnet, N-Mosfet, Arduino nano MCU, hall-effect sensor and an inductive sensor.

3.3 Modeling & Assembly

The gripper was modeled using Autodesk Fusion 360 CAD software and consists of 5 basic 3D printed modules shown in Fig. 3.7:

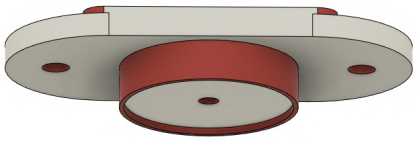

(a) The gripper base with holes for the proximity sensor and electromagnet with embedded hall sensor

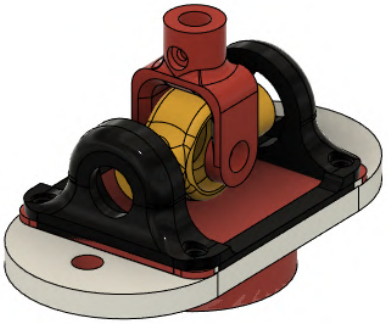

(b) The mount that connects the upper portion of the gripper with the base (black)

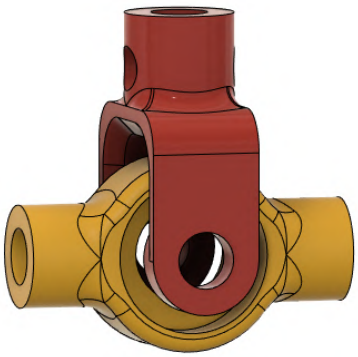

(c) Housing that connects the shaft to the base and housing that accommodates ball bearings and attaches to the gripper and together provides 2-DOF

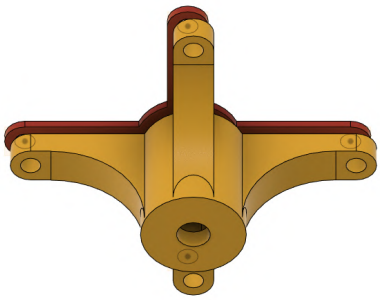

(d) The mount with spring for dampening and which connects to the UAV

Figure 3.7: Modules of the gripper

The gripper has a few components (Sec. 3.2) including sensors and MCU which can be assembled or soldered to each other by hand and assembled together to the 3D printed parts (1-5) by using some screws, nuts and short cylindrical[2] inserts (a-g).
All the components and the final assembled product are shown in (3.8)(3.9).

Figure 3.8: All mechanical components of the gripper

[2]a - ball bearings; b - a metal rod with hex end; c - compression spring; d - cylindrical inserts; e - threaded bolt; f - M6 screw; g - two nuts

3.4 Comparison of tested prototypes

Parameter	EPM Design	Dual Design	Rigid Design	Proposed Design
Weight	250 g	580 g	350 g	400 g
Max Rated Payload	15 kg	80 kg	50 kg	40 kg
Max Shear Payload	2.25 kg	12 kg	7.5 kg	6 kg
Max Tested Payload	500 g	1.5 kg	2.3 kg	4 kg
Feedback	Single	Multiple	Single	Multiple
Scalable	No	Yes	Yes	Yes
Mechanical Design	3-DOF	2-DOF	0-DOF	2-DOF
Power Consumption	≈ 100 mW	≈ 23 W	≈ 20 W	≈ 11.65 W
Cost	≈ 146 Euros	≈ 35 Euros	≈ 15 Euros	≈ 20 Euros

Table 3.1: Comparison between the tested gripping systems

From the comparison table 3.1, we can observe that the optimal grasping mechanism in terms of hold strength vs. power consumption is the proposed 2-DOF gripper design as its payload requirements meet our criterion in the context of the MBZIRC 2020 challenge (Sec. 1.3.1).
The mechanical design of the gripper is reasonable and does not contain any unnecessary elements that add to the weight. The power consumption, though is greater than the EPM solution, is reasonable considering the decreased cost and increased grasping strength and is significantly lower than the power consumption of the UAV.

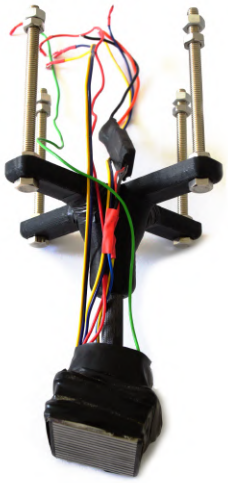

(a) gripper used for MBZIRC 2017

(b) proposed gripper for MBZIRC 2020

Figure 3.9: Comparison between the previous gripper and proposed gripper

(a) Previously used EPM gripper grasping a 0.5 kg metal disk

(b) Proposed gripper grasping a 1.6 kg brick

Figure 3.10: Side by side comparison of the grippers in outdoor test flights

Chapter 4

Feedback and Control

Contents

Reliably detecting whether a payload is actually grasped and onboard the UAV is one of the most crucial tasks for aerial grasping and manipulation.
There have been numerous works where the information about such payload coupling is estimated through the control of the drone wherein the controller detects the increase in the mass of the UAV system and compensates for this mass by varying thrust. Additionally, it is also possible to compensate for a swinging payload under the UAV and stabilize it through the controller [40][43][41]. This method however, becomes more challenging as the payload mass starts to become comparable with the UAV's mass while considering that the UAV must actually grasp the brick for the controller to estimate the mass gradually and requires fine tuning to be practical enough to be employed in time constrained scenarios.

For our task, it is critical to know whether the brick has been successfully grasped almost immediately as the UAV has to fly the payload to the wall area without delay.
In case the grasp was unsuccessful, the UAV must try again to grasp the brick or decide to abandon the brick altogether. These decisions will be made on a higher level by a state machine that runs in the UAV's onboard computer (Sec. 5.1). We shall discuss various sensing and estimation techniques for feedback to explore all possibilities and choose the optimal one for the purposes of our task.

4.1 Feedback with ultrasonic sensors

The first sensor tested was the HC-SR04 ultrasonic sensor (Fig. 4.1 from [44]) with sensing range of 2 cm - 4 m and sensing accuracy of ± 3 mm[1]. Two sensors were tested with the first gripper prototype which had a longer body and hence was mounted on the sides of the long body as shown in Fig. 3.2.
The ultrasonic sensor works on 5 V which can by supplied from the Arduino and by a trigger and echo function. The trigger pin controls the transmitter which transmits ultrasonic pulses at 40 kHz for 10 microseconds and waits for the reflection after hitting an object and is then received by the receiver (Fig. 2.3).
The sensor then returns the duration it took and knowing the speed of sound in air, we can calculate the distance to the detected object (Eq. 2.3). During preliminary test flights,

Figure 4.1: HC-SR04 ultrasonic sensor

it was observed that the raw distance data calculated from the sensors were too noisy to be used for accurate feedback. This was due to the fact that the ultrasonic sensor is not a good instrument to accurately measure distances onboard a flying UAV as the sensor itself has small delays due to the limitation of the speed of sound.
Nevertheless, we chose to prototype with the sensor because it was low cost, small-sized and could be used onboard the gripper easily. However, there are far better and more expensive ranging devices available on the market like the onboard laser based Garmin rangefinder[2] which is used by our UAV system for altitude measurements. As light based ranging techniques are much faster, it would be more suitable for applications onboard a UAV rather than the used ultrasonic sensor.
The noisy raw distance data from the sensors had to be filtered in order to get accurate distance data and feedback. The graphs (Fig. 4.3) and (Fig. 4.4) show the calculated distances from the sensors before and after median filtering with a window size of 20 samples.

[1]Sensor Data sheet - `https://www.electroschematics.com/hc-sr04-datasheet/`
[2]Garmin LIDAR-Lite V3 - `https://buy.garmin.com/en-US/US/p/557294`

The algorithm (Fig. 4.2) used for detection of successful grasping with an ultrasonic sensor is as follows.
The distance[3] in cm is calculated from the ultrasonic sensor and a measurement of 20 samples are median filtered to produce a single final distance value. The median filter is a filter used to remove "out of range" noise from a signal as in the case with our ultrasonic sensor. The filter works by sliding through the signal using a window and replacing the neighbours in the window with the median of the neighbours. The window size for the median filter selected experimentally was 20 samples and implemented in the firmware of the Arduino.
Once the UAV grasps a brick, the drop (Fig. 4.3) (Fig. 4.4) in the distance at that instance is compared to a known threshold of 4 cm which is the minimum possible distance when the gripper touches a flat surface completely and hence was the minimum distance possible should the gripper grasp a brick.

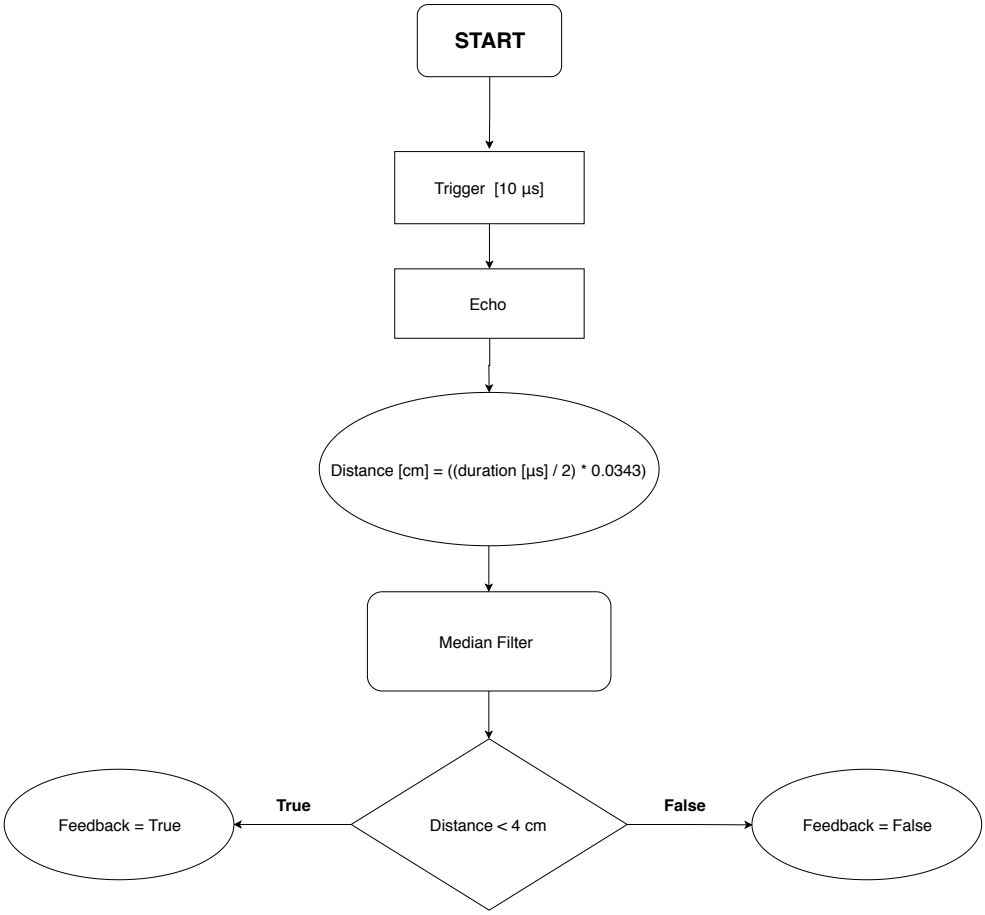

Figure 4.2: Feedback algorithm using ultrasonic sensors

[3]The distance is given by the product of the duration taken for single side transmission multiplied by the speed of sound in air in cm/μs ≈ 0.0343

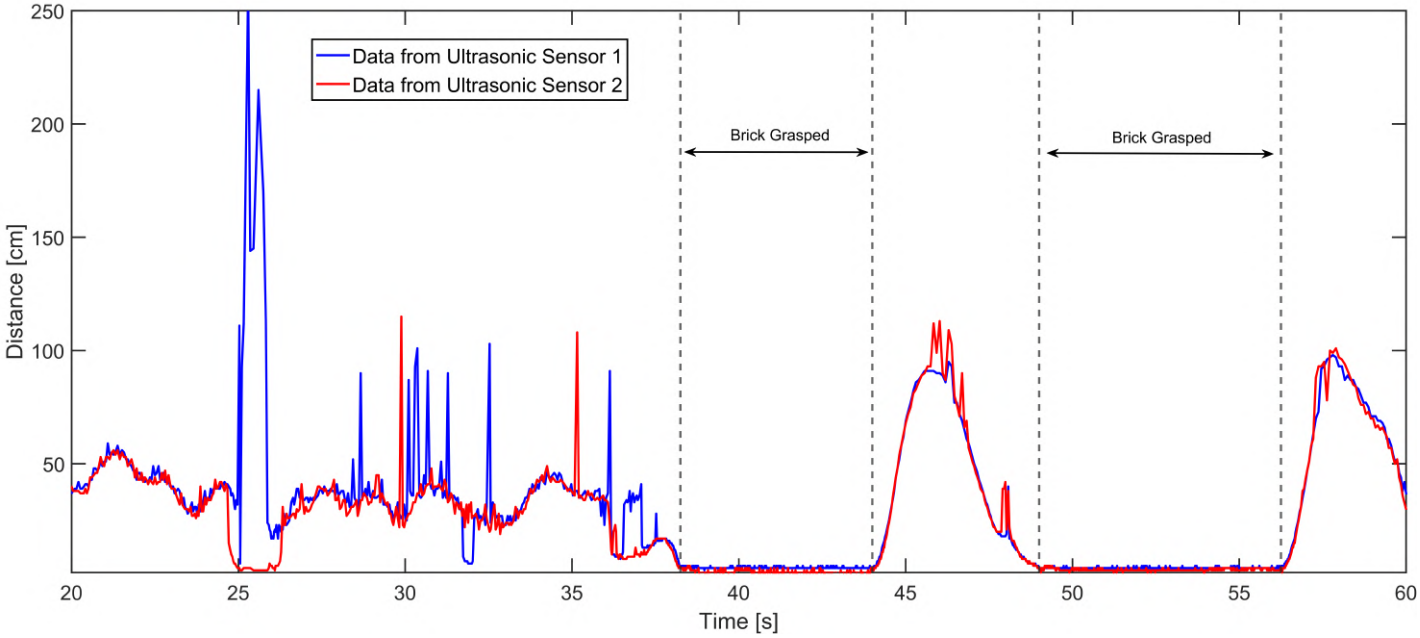

Figure 4.3: Unfiltered distance data from ultrasonic sensor during test flight

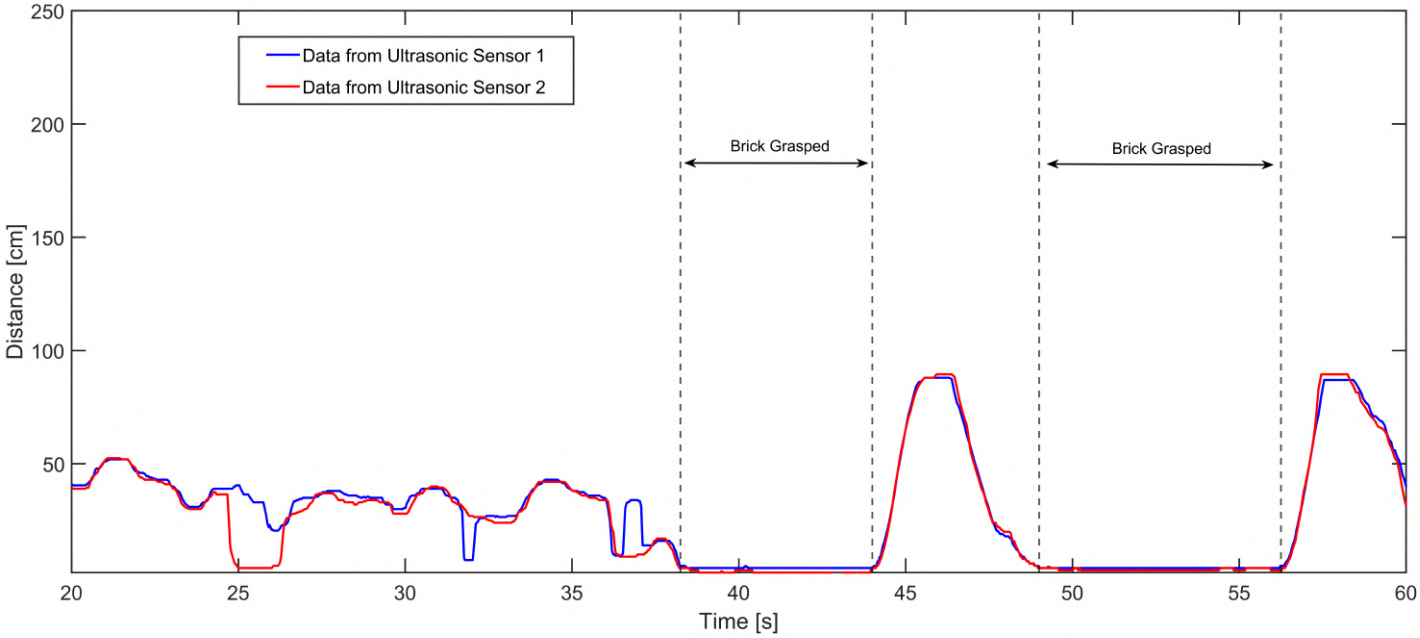

Figure 4.4: Median filtered distance data from ultrasonic sensor during test flight

4.2 Feedback with hall-effect sensors

The sensor tested was the honeywell SS-49e[4]. An analog linear hall effect sensor which uses a linear sourcing output voltage set by the supply voltage and varies it in direct proportion to the strength of the magnetic field. The sensor works on 5 V supplied from the arduino and was embedded into the electromagnet's surface for maximum sensitivity (Fig. 4.5).

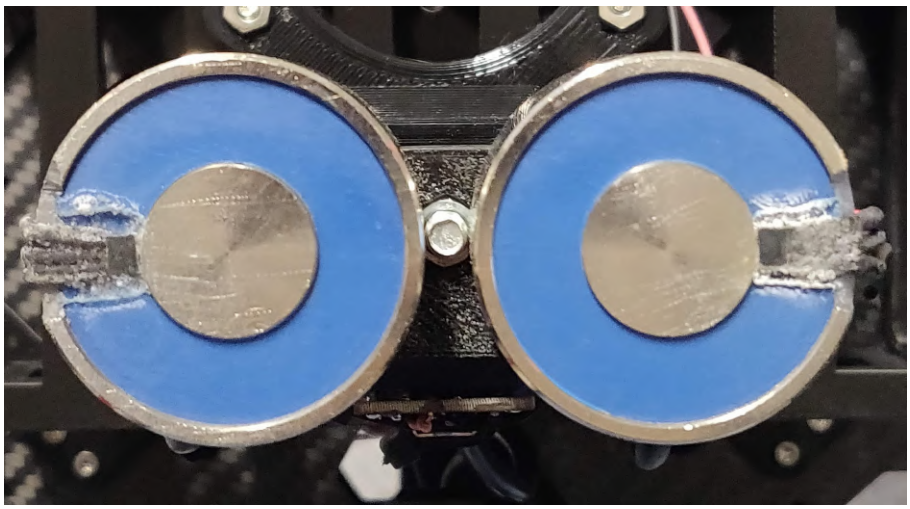

Figure 4.5: Hall sensors embedded in the electromagnet surface

The electromagnet, when powered, has a steady magnetic field provided that there are no parasitic fields in its close vicinity. When a ferrous object is grasped, this magnetic field is changed and the change is directly proportional to the thickness of the ferrous surface.
By using the hall-effect sensor near the electromagnet, we can clearly detect this change in the magnetic field when a ferrous object is grasped.
The Arduino MCU does exactly that by measuring 50 samples and mean filtering them to smooth out the noise caused due any other magnetic anomalies. After filtering, a threshold is calculated and the final feedback is estimated by comparing the calculated threshold before the brick was grasped to the current measured value. In our particular case, there was a drop in the output voltage by the hall sensor when an object was grasped (Fig. 4.7).

The drawback with using this technique is that the hall sensor drifts due to the temperature variation caused by heating of the electromagnet and is easily affected by parasitic fields and requires to be calibrated by measuring some samples and mean filtering them before each grasp.

[4]SS49e Data sheet - `https://sensing.honeywell.com/SS39ET-linear-and-angle-sensor-ics`

4.3 Feedback with inductive sensors

The inductive sensor used[5] is an off the shelf industrial proximity sensor with 8 mm diameter and 5 cm height commonly used in 3D printers for sensing proximity to build plate. It is lightweight, noise resistant and easy to work with (Fig. 4.6 from [45]). It outputs a digital high signal when there is no ferrous object near its proximity and switches to a digital low signal when a ferrous object is bought near it. The feedback for the inductive

Figure 4.6: The used inductive proximity sensor

sensor is the most straight forward as it outputs a constant zero when a brick is grasped by the gripper (Fig. 4.8). The algorithm just checks if the feedback from the inductive sensor is zero and provides the feedback.
There were no major disadvantages using this sensor as it came with a noise filtering circuit out of the box and is widely used for industrial sensing of ferrous objects. However, the position of the sensor must be 2 mm or less from the surface of the ferrous brick to be grasped and in comparison with the hall sensors which have to be "embedded" into the magnet by modifying it, using the proximity sensor is easier. This was usually done while assembling the gripper in a one time calibration and to ensure that the sensor didn't move during flight it was fixed in place using hot-glue.
Two different sensors with sensing distances of 8 mm and 2 mm were tested and the smaller proximity sensor with the sensing distance of 2 mm was found to be sufficient for our task as the sensor only required a one time position calibration.
The raw output from the hall-effect (Fig. 4.7) and inductive (Fig. 4.8) sensors and their corresponding feedback were obtained during experimental outdoor test flights.

[5]The sensor used is the LJ8A3-2-Z Inductive Proximity Sensor

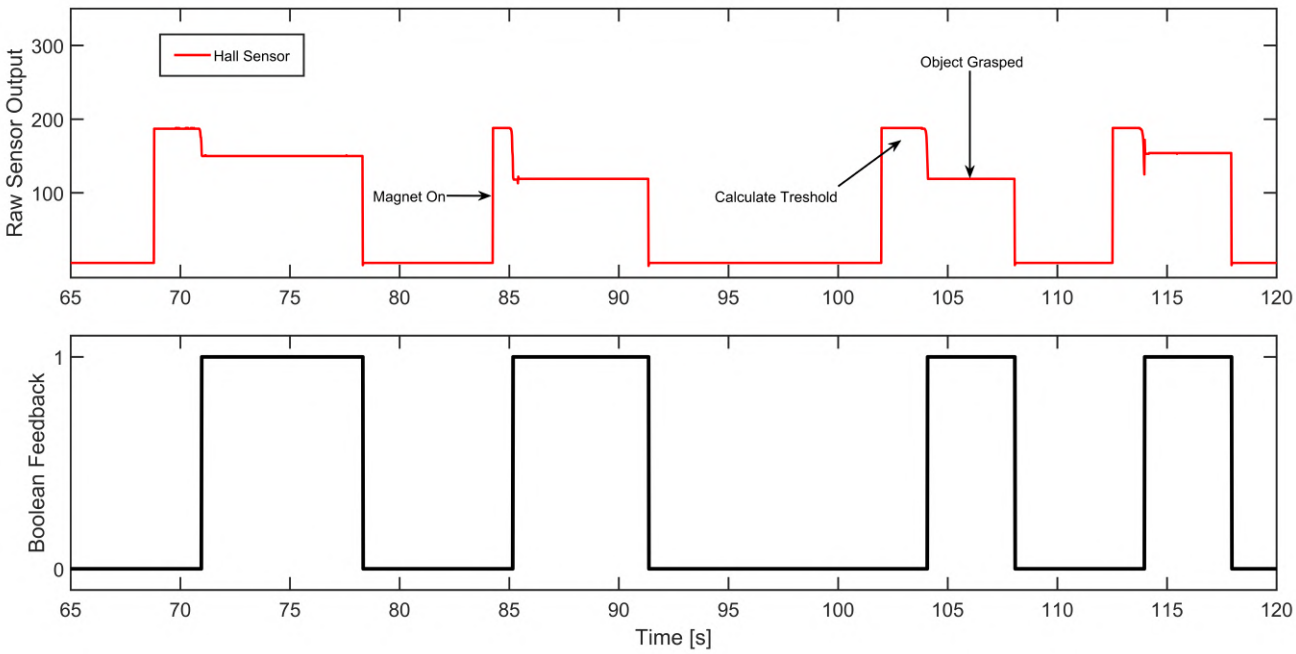

Figure 4.7: Raw data from Hall-Effect sensor and feedback during test flight

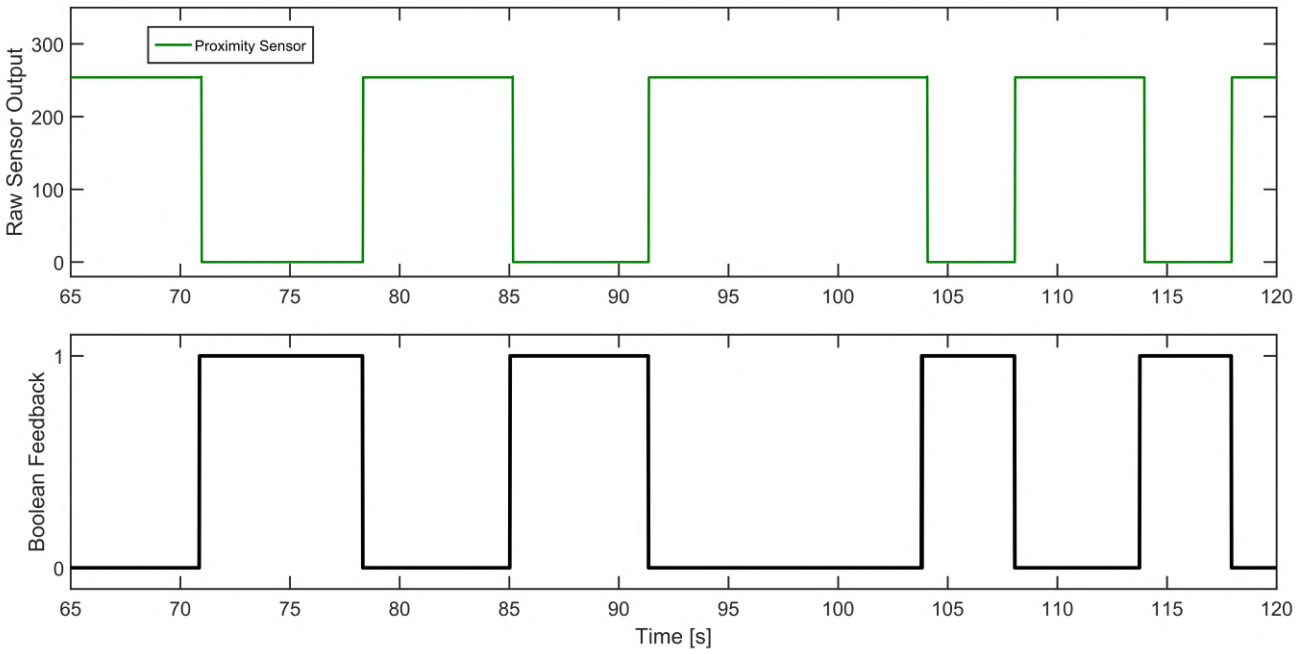

Figure 4.8: Raw data from Inductive proximity sensor and feedback during test flight

4.4 Fusion of feedback methods

We have discussed the implementation and feedback technique for each of the sensors above and also their advantages. Nevertheless, a major drawback of using a single type of sensing technique is that if there is any interference or failure and the primary sensor system is compromised, it cripples the entire system's ability to function as it was designed. As an example, a lot of aviation and robotic systems use redundant measurement or sensing techniques to ensure that the entire system can function properly even if some sensors fail or are compromised due to jamming or interference.

Using this concept as a motivation, we propose using a combination of the hall effect and inductive proximity sensor (Fig. 4.9) as together they provide the necessary redundancy required and estimate the feedback using two independent sensing techniques making the feedback obtained even more reliable. With our implementation, it is possible to obtain the combined feedback from both the sensors using OR logic to determine final feedback or feedback from any individual sensor and use it in ROS. Furthermore, there is diagnostic data with raw measurements and feedback states for easy fault detection and debugging. The estimation algorithm running onboard the MCU is shown in the flowchart Fig. 4.10.

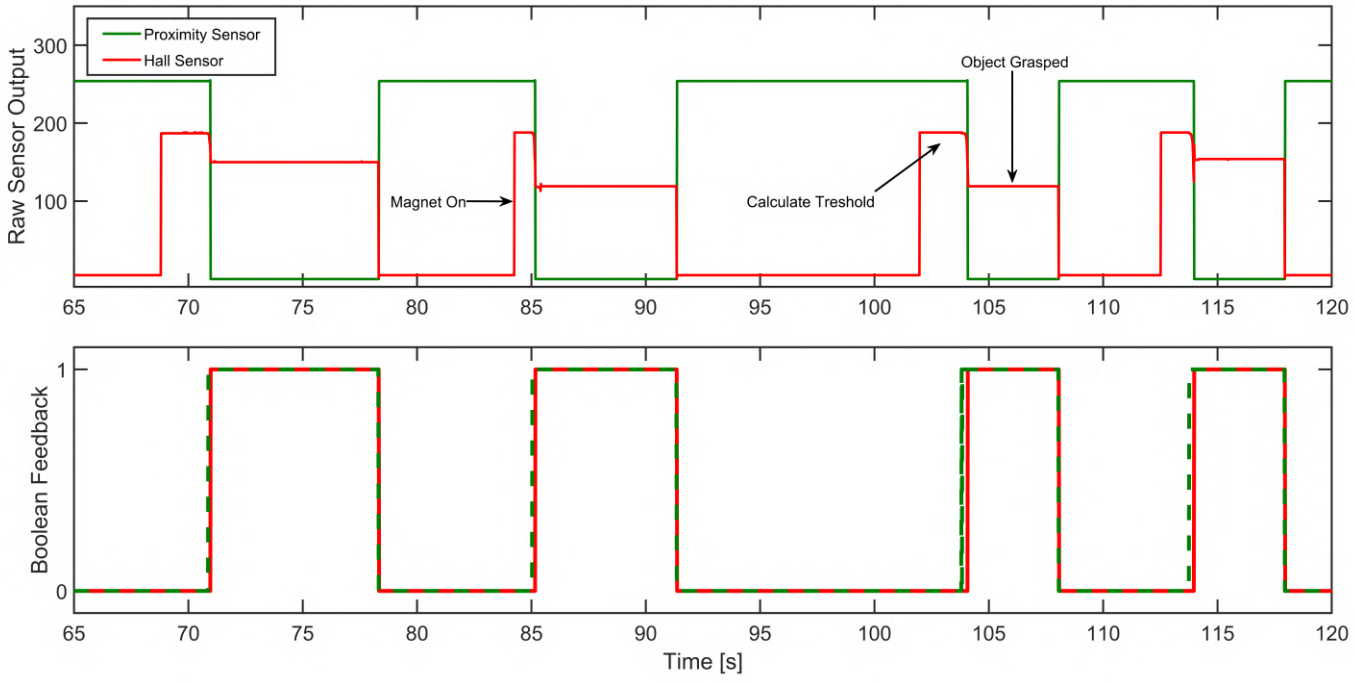

Figure 4.9: Combined data from proximity & hall sensor and feedback during test flight

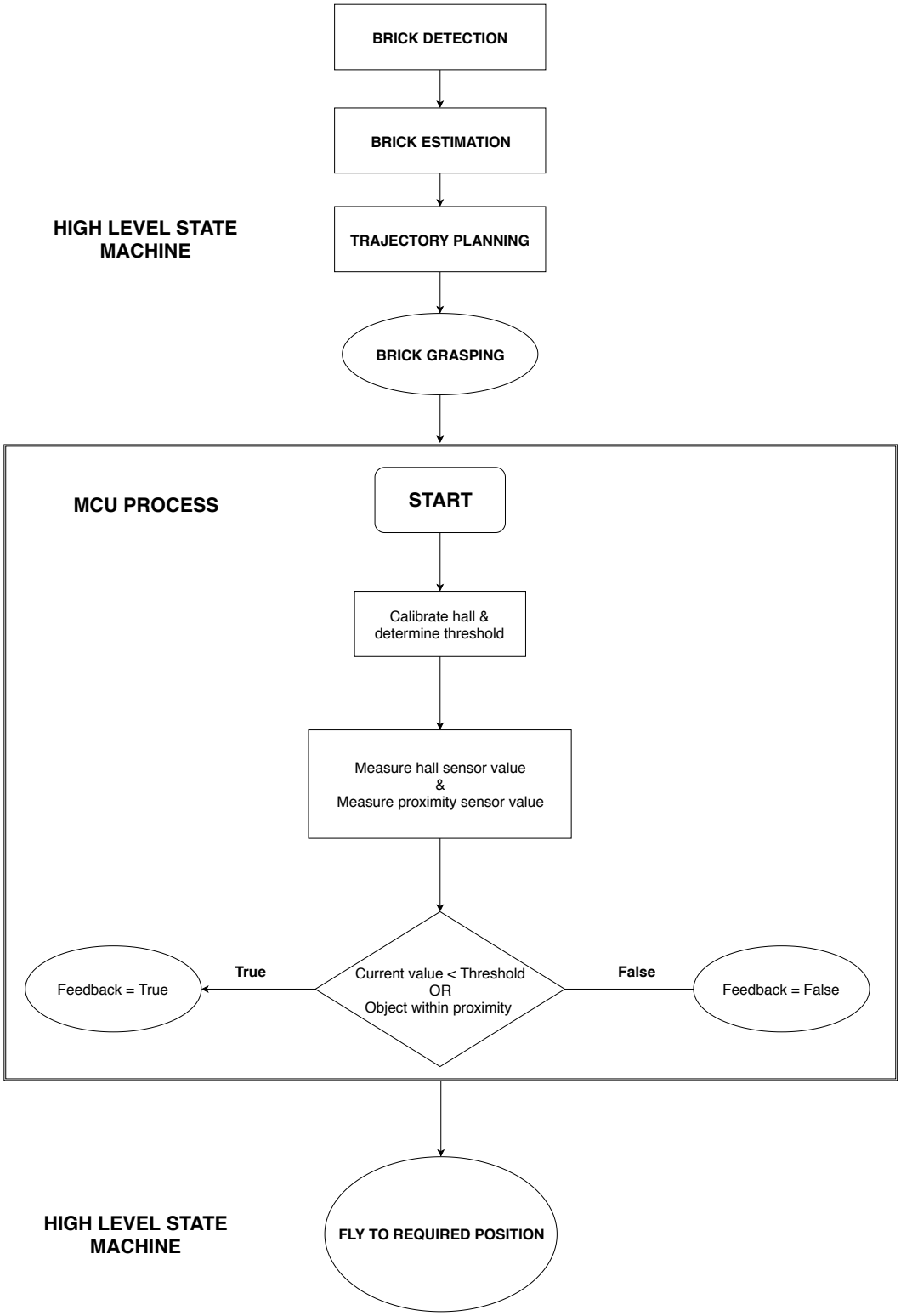

Figure 4.10: Algorithm running onboard the MCU and high level processes

4.5 Gripper control

Control Circuit

The gripper is controlled with a help of a custom designed switching circuit [46] consisting of a N-MOSFET and protective flyback diode [30] that provides the switching action for the electromagnet by a digital signal from the MCU. For prototyping and for the purpose of this thesis, the Arduino MCU with an ATmega328 microprocessor is used for processing the signals from the sensors and providing the control of the electromagnets. But for the competition a custom designed STM 32 MCU board by the MRS group will be used that will provide all the necessary functions for the control and feedback processing of the gripper.

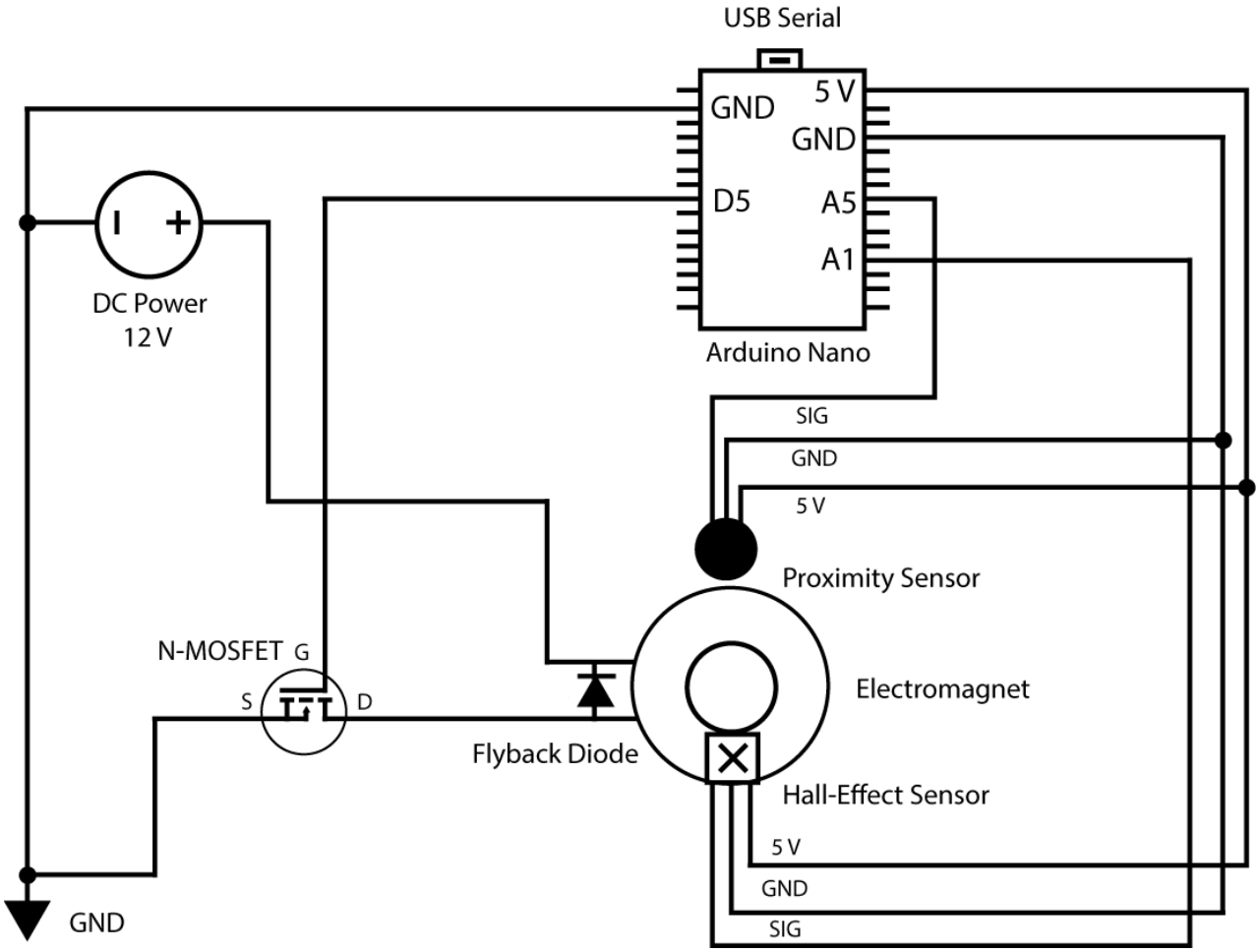

Figure 4.11: Electrical schematic of the gripper circuit

Serial communication

The communication between the gripper and the onboard computer on the UAV is facilitated by a custom "MRS Serial" protocol using an USB cable plugged into the onboard computer.
Messages transmitted and received via this protocol consist of 8-bit values following the rules of UART communication. The protocol is illustrated in Fig. 4.12.

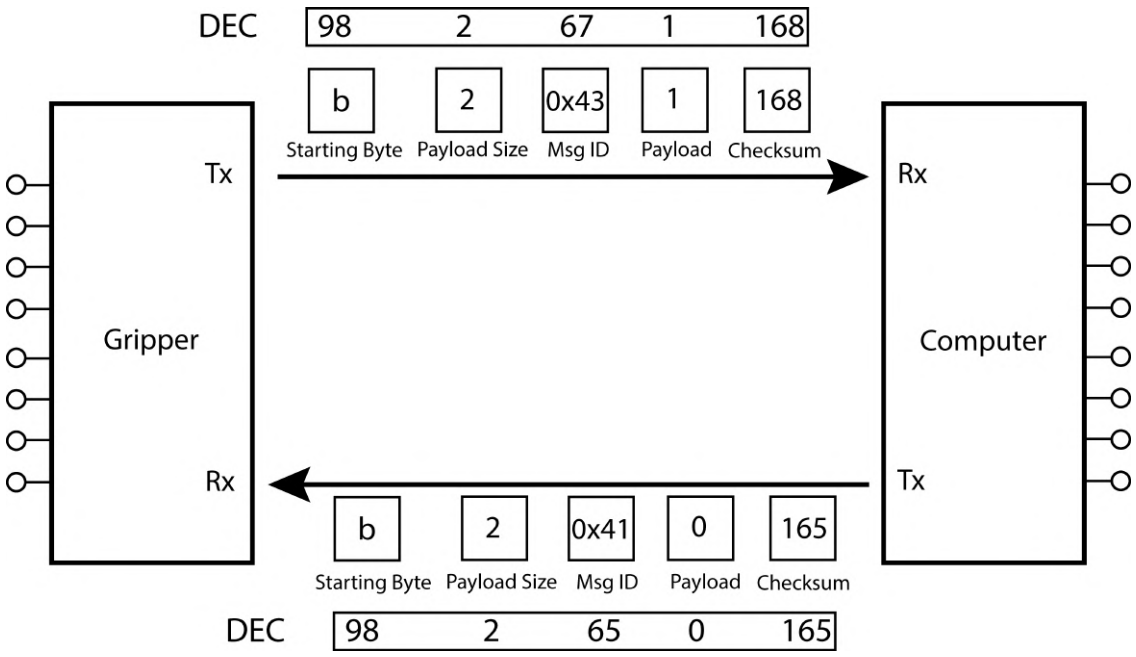

Figure 4.12: Description of the serial protocol

Each character inside the box represents one 8 bit value. The first byte is always the character "b", this represents the start of a serial message. The next byte written is the payload size. Payload of the message can range from 1 to 256 bytes long and the first byte of the payload is the message id, which is pre-defined and serves to differentiate between different messages of the same length. The message id is followed by the payload and finally, the checksum is calculated by the sender by summing the 8-bit data stream and compared at the receiving end. If the checksums do not match, the message is discarded. This is summarized in (table 4.1).

Byte	function
b	Message start
Payload size	Size of the expected message
Message ID	Identifier that ensures messages are parsed correctly
Payload	Actual message
Checksum	Ensures messages are not corrupted or incomplete at the receiving end

Table 4.1: Serial bits and their function in used protocol

ROS Node

A ROS node runs on the onboard computer and is integrated into the software pipeline of the UAV's system. This node publishes diagnostic information about the gripper for easier debugging and also publishes the feedback from the gripper via ROS topics.
The gripper is controlled by ROS services that allows for the control of the electromagnet and also sensor calibration in the case of the hall sensor. A table of the functions provided by the ROS node and their message IDs for serial communication is shown below (table 4.2):

Name	Type	Purpose	Message ID
Grip	ROS Service	Turn the gripper ON and calibrate onboard sensors	0x40
Ungrip	ROS Service	Turn the gripper OFF	0x41
gripper_diagnostics	ROS topic	Provide diagnostic information from sensors such as raw values and gripper state	N/A
gripper_feedback	ROS topic	Provide final boolean feedback	N/A

Table 4.2: Implemented functions facilitated by ROS

The switching control of the gripper is provided by two ROS services (Sec. 2.1) "grip" and "ungrip" which turns the electromagnet on and off respectively by providing a high or low signal to the MOSFET (table 4.2). The calibration of the hall sensor is done automatically when the "grip" ROS service is called which is performed by the state machine after an object is detected and the UAV descents to grasp it. The gripper diagnostics topic publishes information for debugging such as the current state of the gripper, the measured raw sensor values and feedback from the individual sensors. The gripper feedback provides a final estimation to the drone which is a boolean value.

Chapter 5

Outdoor Experiments

Contents

In order to experimentally validate the proposed idea for an aerial grasping mechanism, we conducted a series of experiments [1][2] under both indoor and outdoor conditions where the UAV system for challenge II of MBZRIC 2020 along with the grasping mechanisms were tested thoroughly.
In this chapter, an overview of the entire system under development for the competition and the experimental data from the test flights are presented.

5.1 Overview of UAV system

Hardware Architecture

The proposed UAV platform is a complex system with multiple onboard sensors and computational units shown in Fig. 5.1. The open-source nature of the system makes it ideal for rapid prototyping which in turn makes them perfect for competition scenarios and multi-robot system research.
The hardware components are selected with certain factors such as payload, reliable sensor data and computational power in mind. The UAV frame selected is the tarot 650 sport quad-copter with carbon fiber frame making it lightweight while satisfying the size requirements given for the MBZIRC 2020 competition.

[1] Autonomous grasping test: `https://youtu.be/WBgUNp1UqlA`
[2] Piloted grasping test: `https://youtu.be/bOQ2FRhOzXw`

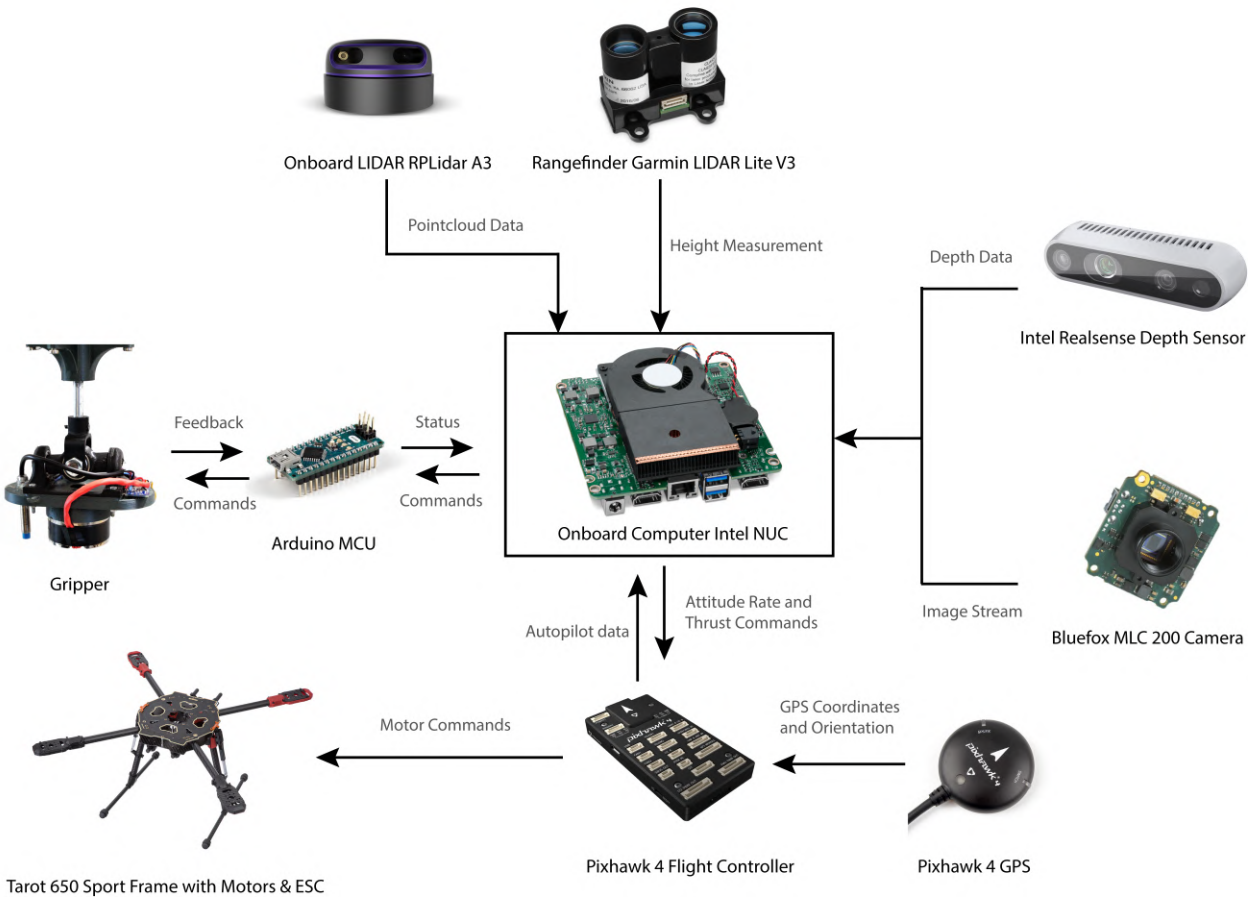

Figure 5.1: Hardware architecture

The system is controlled at the lowest level by a Pixhawk 4 flight controller with its own GPS that provides reliable coordinates and contains various sensors such as gyroscopes, accelerometers, magnetometers and barometer.
An Intel NUC-i7 computer provides the necessary computational power required to solve the image processing, signal processing, state estimation, feedback control, motion planning and UAV coordination tasks effectively. The communication between the computer and the Pixhawk controller is done with the MAVlink protocol and communication between the UAVs in a group is achieved with the help of the WIFI module on the NUC computer. Two Bluefox MLC 200 cameras are used for challenge II onboard the UAV, one running an optic flow [47] algorithm that provides odometry during navigation and the other fitted with a fisheye lens that provides a wider field of view in the detection for brick grasping [48] while the LIDAR is used for localization [16] of the UAV and mapping of the environment. The Intel realsense depth camera will be used conditionally if the task requires it, for example in the case of assembly of the wall in challenge II or in challenge III where a group of UAVs must extinguish a series of fires in a simulated urban fire-fighting scenario.

While the pixhawk controller provides barometric altitude readings, the UAV does not have any information about the distance to a detected brick or the ground from the pixhawk. This is solved by the garmin lite v3 rangefinder which provides distance to ground readings in realtime.
Finally, the gripper communicates information about the feedback status with the computer with the help of an Arduino nano MCU running a custom serial protocol described in (Sec. 4.5) and can be controlled via the serial protocol for grasp and release of an object.

System Software Pipeline

The software used for the UAVs utilizes the open-source Robot Operating System (ROS) running on the Intel NUC computer in which each task and sub-tasks can be split into smaller manageable structures in ROS (Nodes). All software changes are rigorously tested in Gazebo simulator along with the firmware from Pixhawk as this provides a realistic test-bed for our systems minimizing crashes and increasing safety during field tests.

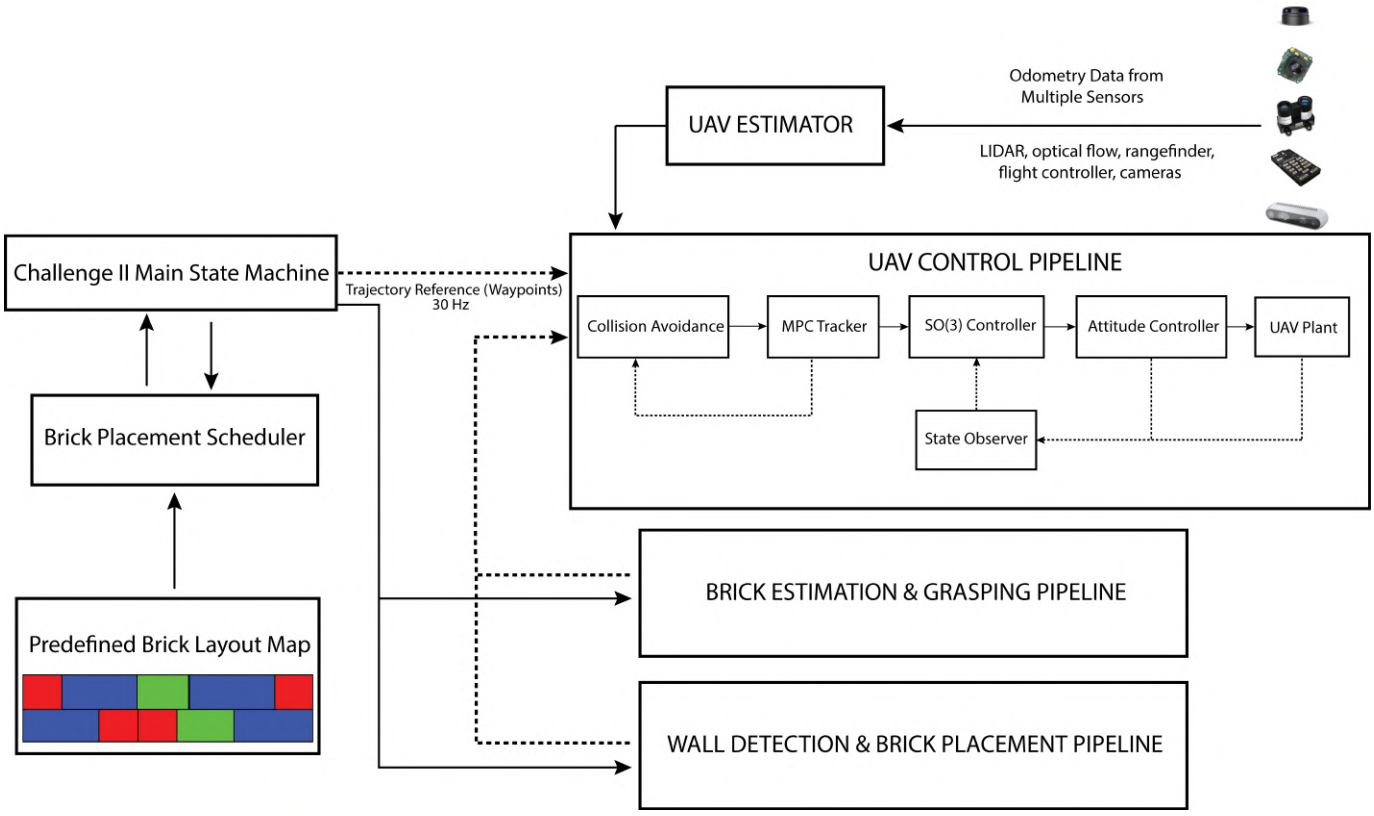

Figure 5.2: Overview of software pipeline

An overview of the system pipeline is illustrated in Fig. 5.2. The main core of the system consists of a state machine which is used to manage all sub-systems and asynchronously

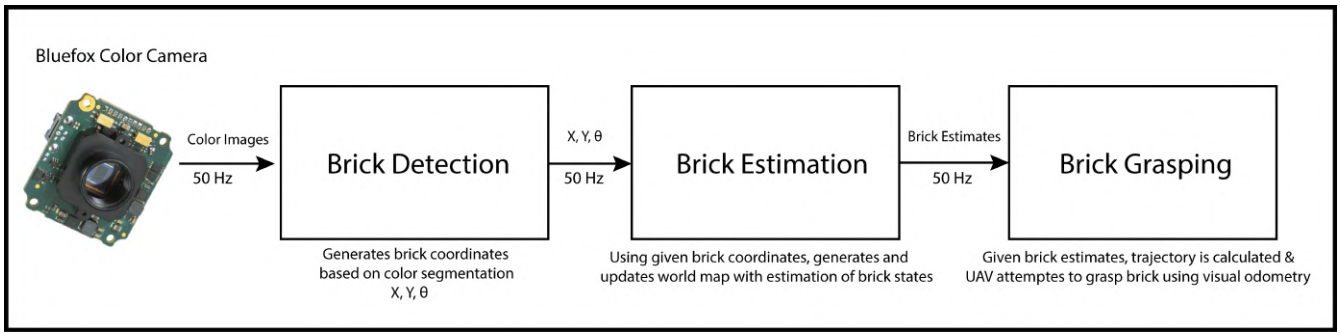

Figure 5.3: Sub-Pipeline for autonomous grasping

multiplexes between different sub-pipelines as required depending upon a particular task, which in our case corresponds to challenge II. The state machine is designed with the help of FlexBE (Python Library) and is fully integrated into the designed ROS system framework [49].

The state machine, in the first step is fed information from a brick placement scheduler which relays information about each brick object and its pre-defined parameters such as color, weight and priority. It also contains the order of how each brick must be placed in the wall as prescribed by a plan given to us before the challenge. The second step consists of the state machine performing various sweeps of the competition arena where individual bricks are detected, localized and the scheduler is updated accordingly.

The brick estimation and grasping sub-pipeline is illustrated in Fig. 5.3. As illustrated, the color camera searches the competition arena while running a brick detection algorithm that uses color segmentation [50][48] and navigates during flight on an optical flow algorithm using a grey-scale camera [47]. Once a brick is detected and localized the coordinates of the brick on the ground are calculated and relayed to the brick estimation algorithm which generates the map containing the brick states. The brick estimator keeps track of all the detected bricks in the environment and deactivates or deletes a brick if the grasping is unsuccessful or if the brick is already assembled on the wall.
Once the brick is estimated and trajectory leading to a particular brick is known, the UAV goes to the given coordinates using waypoints and aligns itself horizontally above the estimated position of the brick. It then descends to a height of 1.5 m above the ground. Once the UAV has reached the desired height and is aligned above the brick it tries to grasp the brick by turning on the gripper and descending gently onto the brick surface.
If the brick is successfully grasped the gripper returns positive detection and the UAV ascends to nominal height and flies to the wall-building area where each brick is assembled according to the brick layout map using a depth camera and visual servoing. If the UAV is unable to grasp the brick in 3 attempts, the state machine terminates the process with the outcome that grasping was unsuccessful.

On the low-level, the UAV is stabilized and controlled by the control pipeline [51] shown in Fig. 5.2. Automatic control of the UAVs relies on estimates of the states of the UAV model. The platform is equipped with multiple onboard sensors providing independent localization data and fuses this information to obtain a single and smooth estimate of UAV "pose" which contains both horizontal and vertical position, velocity estimation and is an important criteria as the non-linear SO(3) controller with state feedback is sensitive to noise [51].
The position controller uses the estimated state in a feedback loop to follow the trajectories given to it by the trajectory planner [49].

(a) UAV transporting red brick

(b) UAV transporting green brick

Figure 5.4: The complete system in action during outdoor experimental flights

5.2 Experimental data & observations

Maximum Payload

Multiple experiments were conducted in the Czech countryside in experimental camps by the MRS group where the entire hardware and software system described (Sec. 5.1) was tested. The maximum payload grasped by the gripper system was 4 kg with nominal loads of 1.5 kg - 2 kg and excluding the UAV mass which was around 3 kg. The maximum payloads correspond to the blue and green bricks that are 1.2 m and 0.6 m long.
An important factor to consider is the payload limitations of the UAV system itself as even though the gripper is capable of theoretical payloads up to 6 kg, the first test conducted with the heaviest green brick resulted in a failure due to the low-pitch propellers that did not provide the necessary thrust for the mass of the entire system and had to be changed to propellers with a higher pitch angle which was then successful in lifting the heavier bricks.

Maximum Sustainable Slide

Sudden aerial maneuvers and attitude change by the UAV during flight affect the forces on it's payload and considering that the holding force of electromagnets are especially vulnerable to shear forces acting on it [52][16], we had to experimentally approximate the maximum sustainable slide forces for our grasping mechanism.
The selected electromagnet was tested with lateral pull tests with a weighing scale to measure at what point the payload would slide off the electromagnet. An important parameter here (table 5.1) is the thickness of the ferrous plate as this greatly affects the holding force of the electromagnet [33]. During flight, newton's second law plays a major role in determining the forces acting on the payload during aggressive maneuvers. Therefore, the higher the mass of the payload, the more force acting on it. For the competition, we will restrict the UAV from making aggressive attitude changes and also limit the velocities of the UAV in order to ensure safety and reliability of operation. The experimentally tested values for the maximum sustainable slide are shown in table 5.1.

Brick Color	**Plate Thickness**	**Mass**	**Max Sustainable Slide Force**
Red	0.75 mm	0.75 kg	0.87 kg
Green	1.5 mm	1.37 kg	2.00 kg
Blue	2.00 mm	2.36 kg	4.80 kg

Table 5.1: Test of maximum slide force

Aerial Grasping

The final test we performed were direct grasp and release tests with the UAV and gripper system in both piloted and autonomous flights.
In order to measure the performance of the grasping system during autonomous flight, we took positional measurements when there was a payload attached to the UAV.
The graph (Fig. 5.6) shows the data calculated from the odometry of the UAV and the "set-points" given to the UAV. By subtracting the real positional data from the set-point values, we can calculate the positional control error of the UAV during grasping and transport of the bricks. From (Fig. 5.7), we can observe that the set-point position error of the UAV during flight does not exceed 20 cm even with payload coupling. Taking into consideration that the UAV controller design is robust enough for such aerial grasping tasks, this is a good metric to measure the performance of our proposed grasping mechanism and show that it does not cause major disturbances to the UAV system.

(a) The UAV hovers while placing the green brick

(b) UAV flies above the wall with the red brick

(c) UAV grasps pliers showing the versatility of the gripper

(d) UAV attempts to place the red brick on the wall

Figure 5.5: Snaps from outdoor experiments where the complete system is tested under the challenge II scenario

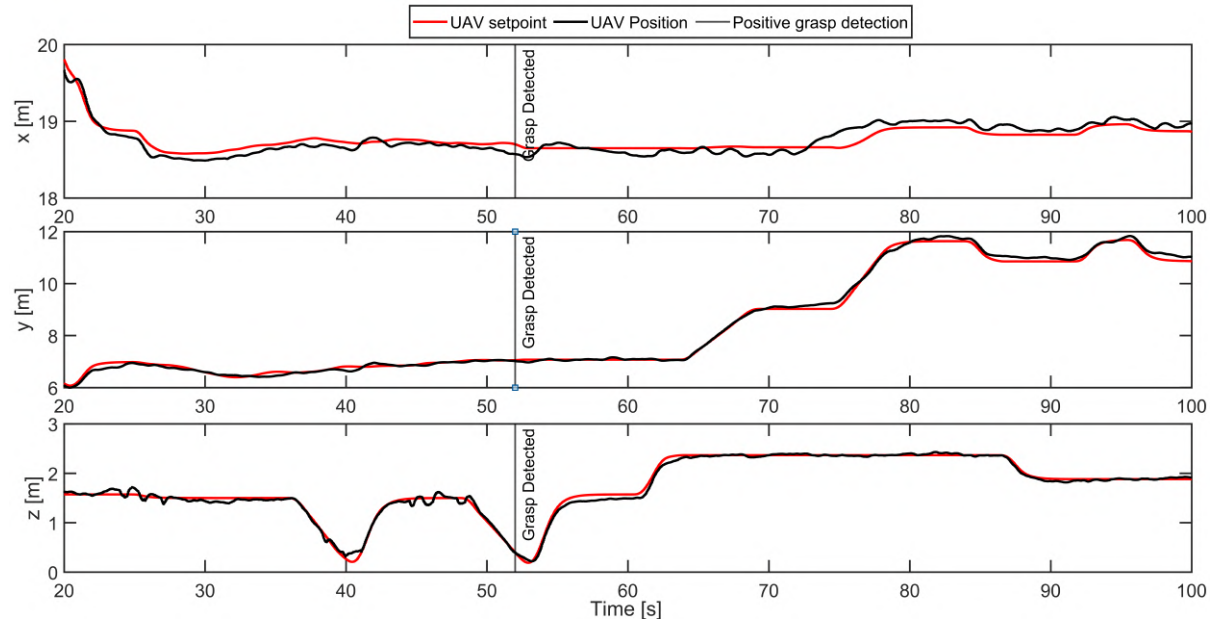

Figure 5.6: UAV positional control during grasping of brick

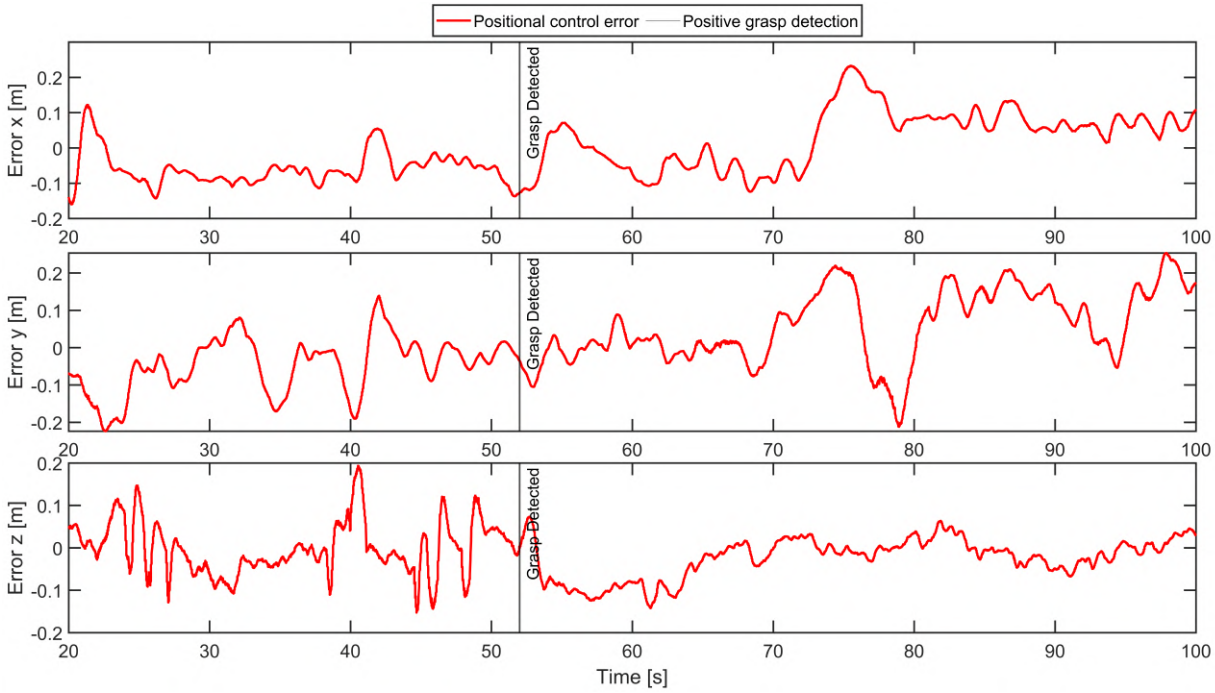

Figure 5.7: Control error during grasping of brick

Chapter 6

Conclusion

Contents

In this thesis, we have developed a novel mechanism for aerial grasping and manipulation by autonomous unmanned aerial vehicles. The proposed final design of the grasping mechanism is a result of many iterations that were tested with test bricks in outdoor experimental test flights as well as indoor conditions. The final design was refined over time and is robust, reliable and has sufficient payload capabilities for a wide variety of ferromagnetic payloads.
An overall description of the UAV system in development for MBZIRC 2020 competition and the integration of the grasping mechanism with the system is also discussed.
According to the formal assignment of this bachelor's thesis, the following tasks have been completed:

- A novel magnetic based grasping mechanism has been designed and tested with real test bricks as per the MBZIRC 2020 requirements [See chapter 3].
- The feedback system consisting of various sensors was tested and a suitable system along with the estimation algorithm is implemented [See chapter 4].
- The implemented gripper system is integrated with ROS and communicates with the onboard computer to provide an estimate of the feedback status 4].
- Outdoor tests with real experimental data and evaluation of the tested systems are provided and discussed [See chapter 5].

6.1 Future work

Autonomous aerial grasping by UAVs is becoming a widely studied topic in the field of aerial robotics. However, the current state of the art in UAV technologies is limited due to limitations in battery technology and onboard processing power. In the coming years, as battery technologies improve and more off the shelf products for aerial robotics emerge, UAVs will be more practical to employ for long-range tasks as well as aerial manipulation tasks of heavier payloads.

During the development of this thesis, several ideas were experimented with such as adding some actuation to the 2-DOF gripper using servos to align the payload toward the center of gravity and provide better stabilization or using springs for passive stabilization. Most of these ideas did not make it to the final presented work due to its impracticality, complexity or deviation from the assigned task.
The presented work can be improved upon by scaling it up for heavier payloads and by implementing a better estimation technique with fuzzy logic or advanced sensor fusion. It is also crucial to have orientation feedback of the payload after grasping it for designing robust flight controllers that are disturbance tolerant. However, this is a challenging task to solve in the real world. Several other innovative ideas can also be used to make the proposed design more robust such as using lighter and stronger materials (e.g. carbon fiber composites) for manufacturing as such materials ensure integrity for long-term uses. Nevertheless, electromagnetic based grasping technologies due to their versatility prove to be strong candidates for the future of UAV based aerial manipulation.

Bibliography

[1] R. Ritz and R. D'Andrea, "Carrying a flexible payload with multiple flying vehicles," in *2013 IEEE/RSJ International Conference on Intelligent Robots and Systems*, Nov 2013, pp. 3465–3471.

[2] N. Michael, J. Fink, and V. Kumar, "Cooperative manipulation and transportation with aerial robots," *Autonomous Robots*, vol. 30, no. 1, pp. 73–86, Jan 2011. [Online]. Available: https://doi.org/10.1007/s10514-010-9205-0

[3] G. Loianno and V. Kumar, "Cooperative transportation using small quadrotors using monocular vision and inertial sensing," *IEEE Robotics and Automation Letters*, vol. 3, pp. 680–687, 2018.

[4] M. Becker and D. Sheffler, "Designing a high speed, stealthy, and payload-focused vtol uav," in *2016 IEEE Systems and Information Engineering Design Symposium (SIEDS)*, April 2016, pp. 176–180.

[5] M. A. Ma'sum, M. K. Arrofi, G. Jati, F. Arifin, M. N. Kurniawan, P. Mursanto, and W. Jatmiko, "Simulation of intelligent unmanned aerial vehicle (uav) for military surveillance," in *2013 International Conference on Advanced Computer Science and Information Systems (ICACSIS)*, Sep. 2013, pp. 161–166.

[6] J. Chudoba, M. Kulich, M. Saska, T. Báča, and L. Přeučil, "Exploration and mapping technique suited for visual-features based localization of mavs," *Journal of Intelligent & Robotic Systems.*, vol. 84, no. 1, pp. 351–369, 2016.

[7] T. Ozaslan, G. Loianno, J. Keller, C. J. Taylor, and V. Kumar, "Spatio-temporally smooth local mapping and state estimation inside generalized cylinders with micro aerial vehicles," *IEEE Robotics and Automation Letters*, vol. 3, no. 4, pp. 4209–4216, Oct 2018.

[8] G. Loianno, J. Thomas, and V. Kumar, "Cooperative localization and mapping of mavs using rgb-d sensors," in *2015 IEEE International Conference on Robotics and Automation (ICRA)*, May 2015, pp. 4021–4028.

[9] T. Tomic, K. Schmid, P. Lutz, A. Domel, M. Kassecker, E. Mair, I. L. Grixa, F. Ruess, M. Suppa, and D. Burschka, "Toward a fully autonomous uav: Research platform for indoor and outdoor urban search and rescue," *IEEE Robotics Automation Magazine*, vol. 19, no. 3, pp. 46–56, Sep. 2012.

[10] N. Michael, S. Shen, K. Mohta, Y. Mulgaonkar, V. Kumar, K. Nagatani, Y. Okada, S. Kiribayashi, K. Otake, K. Yoshida, K. Ohno, E. Takeuchi, and S. Tadokoro, "Collaborative mapping of an earthquake-damaged building via ground and aerial robots," *Journal of Field Robotics*, vol. 29, no. 5, pp. 832–841, 2012. [Online]. Available: https://onlinelibrary.wiley.com/doi/abs/10.1002/rob.21436

[11] A. Nedungadi and M. Saska, "Design of an active-reliable grasping mechanism for autonomous unmanned aerial vehicles," J. Mazal, Ed. Springer, 2020, presented at Modelling and Simulation for Autonomous Systems and Accepted for publication in Springer Lecture Notes in Computer Science, 2020.

[12] "MBZIRC 2020," see: Challenge II, Accessed: 2-9-2019. [Online]. Available: https://www.mbzirc.com/challenge/2020

[13] U. A. Fiaz, M. Abdelkader, and J. S. Shamma, "An intelligent gripper design for autonomous aerial transport with passive magnetic grasping and dual-impulsive release," in *2018 IEEE/ASME International Conference on Advanced Intelligent Mechatronics (AIM)*, July 2018, pp. 1027–1032.

[14] J. Lee, D. H. Shim, S. Cho, H. Shin, S. Jung, D. Lee, and J. Kang, "A mission management system for complex aerial logistics by multiple unmanned aerial vehicles in mbzirc 2017," *Journal of Field Robotics*, vol. 36, no. 5, pp. 919–939, 2019. [Online]. Available: https://onlinelibrary.wiley.com/doi/abs/10.1002/rob.21860

[15] A. R. Castaño, F. Real, P. Ramón-Soria, J. Capitán, V. Vega, B. C. Arrue, A. Torres-González, and A. Ollero, "Al-robotics team: A cooperative multi-unmanned aerial vehicle approach for the mohamed bin zayed international robotic challenge," *Journal of Field Robotics*, vol. 36, no. 1, pp. 104–124, 2019. [Online]. Available: https://onlinelibrary.wiley.com/doi/abs/10.1002/rob.21810

[16] G. Loianno, V. Spurny, T. Baca, J. Thomas, D. Thakur, T. Krajnik, A. Zhou, A. Cho, M. Saska, and V. Kumar, "Localization, grasping, and transportation of magnetic objects by a team of mavs in challenging desert like environments," *IEEE Robotics and Automation Letters*, vol. 3, no. 3, pp. 1576–1583, 2018.

[17] R. Bahnemann, M. Pantic, M. Popovic, D. Schindler, M. Tranzatto, M. Kamel, M. Grimm, J. Widauer, R. Siegwart, and J. Nieto, "The eth-mav team in the mbz international robotics challenge," *Journal of Field Robotics*, vol. 36, no. 1, pp. 78–103, 2019. [Online]. Available: https://onlinelibrary.wiley.com/doi/abs/10.1002/rob.21824

[18] A. Gawel, M. Kamel, T. Novkovic, J. Widauer, D. Schindler, B. P. von Altishofen, R. Siegwart, and J. Nieto, "Aerial picking and delivery of magnetic objects with mavs," in *2017 IEEE International Conference on Robotics and Automation (ICRA)*, May 2017, pp. 5746–5752.

[19] P. Kohout, "A system for autonomous grasping and carrying of objects by a pair of helicopters," 2017, Master Thesis, Czech Technical University in Prague.

[20] R. Cano, C. Pérez, F. O. Pruaño, A. Ollero, and G. Heredia, "Mechanical design of a 6-dof aerial manipulator for assembling bar structures using uavs," in *2nd RED-UAS 2013 Workshop on Research, Education and Development of Unmanned Aerial Systems*, 2013, pp. 1–7.

[21] G. Jiang and R. Voyles, "Hexrotor uav platform enabling dextrous interaction with structures-flight test," in *2013 IEEE International Symposium on Safety, Security, and Rescue Robotics (SSRR)*, Oct 2013, pp. 1–6.

[22] M. Fumagalli, S. Stramigioli, and R. Carloni, "Mechatronic design of a robotic manipulator for unmanned aerial vehicles," in *2016 IEEE/RSJ International Conference on Intelligent Robots and Systems (IROS)*, Oct 2016, pp. 4843–4848.

[23] P. E. I. Pounds, D. R. Bersak, and A. M. Dollar, "Practical aerial grasping of unstructured objects," in *2011 IEEE Conference on Technologies for Practical Robot Applications*, April 2011, pp. 99–104.

[24] C. C. Kessens, J. Thomas, J. P. Desai, and V. Kumar, "Versatile aerial grasping using self-sealing suction," in *2016 IEEE International Conference on Robotics and Automation (ICRA)*, May 2016, pp. 3249–3254.

[25] D. Mellinger, Q. Lindsey, M. Shomin, and V. Kumar, "Design, modeling, estimation and control for aerial grasping and manipulation," in *2011 IEEE/RSJ International Conference on Intelligent Robots and Systems*, Sep. 2011, pp. 2668–2673.

[26] ROS, "ROS - Introduction," accessed: 18-11-2019. [Online]. Available: http://wiki.ros.org/ROS/Introduction

[27] Encyclopedia Britannica, inc., "Electromagnet," accessed: 15-11-2019. [Online]. Available: https://www.britannica.com/science/electromagnet

[28] Binder Magnetic, "Technical explanations for holding magnets: Electromagnetic holding magnets, accessed: 15-11-2019. [Online]. Available: https://www.binder-magnetic.com/documentation/technical-explanations-for-holding-magnets/?lang=en

[29] Kendrion, "Technical definitions: The holding magnet," accessed: 15-11-2019. [Online]. Available: https://www.kendrion.com/industrial/ims/fr/competences/technical-explaination/the-holding-magnet.html

[30] T. Agarwal, "Flyback diode," accessed: 15-11-2019. [Online]. Available: https://www.elprocus.com/freewheeling-or-flyback-diode-circuit-working-functions/

[31] Kendrion, "Technical definitions: The electromagnet," accessed: 27-11-2019. [Online]. Available: https://www.kendrion.com/industrial/ims/en/competences/technical-explaination/the-electromagnet.html

[32] Wikipedia, "Remanence," accessed: 27-10-2019. [Online]. Available: https://en.wikipedia.org/wiki/Remanence

[33] Goudsmit Magnetics, "Goudsmit - hold-force curve with plate thickness," accessed: 15-11-2019. [Online]. Available: https://www.goudsmitmagnets.com/data/repository/documents/Forces_GM17804.pdf

[34] Innover Bot, "Hc-sr04 ultrasonic sensor," accessed: 12-26-2019. [Online]. Available: https://www.rima-technology.com/2017/07/23/ultrasonic-sensor-hc-sr04-arduino/

[35] Electro Schematics, "Inductive proximity working," accessed: 12-26-2019. [Online]. Available: https://www.electroschematics.com/inductive-proximity-switch-w-sensor/

[36] Electronics Tutorials, "Hall effect sensor working principles," accessed: 12-23-2019. [Online]. Available: https://www.electronics-tutorials.ws/electromagnetism/hall-effect.html

[37] P. Jaiswal, "Demystifying drone dynamics!" accessed: 21-11-2019. [Online]. Available: https://towardsdatascience.com/demystifying-drone-dynamics-ee98b1ba882f

[38] U.S. Department of Transportation (FAA), "Helicopter flying handbook," see: Chapter 02 - Aerodynamics of flight, Accessed: 22-11-2019. [Online]. Available: https://www.faa.gov/regulations_policies/handbooks_manuals/aviation/helicopter_flying_handbook/

[39] NASA Glenn Research Center, "Beginner's guide to aerodynamics," see: Description of lift, Accessed: 12-23-2019. [Online]. Available: https://www.grc.nasa.gov/www/k-12/airplane/lift1.html

[40] B. Lee, H. Lee, D. Yoo, G. Moon, D. Lee, Y. Kim, and M. Tahk, "Study on payload stabilization method with the slung-load transportation system using a quad-rotor," in *2015 European Control Conference (ECC)*, July 2015, pp. 2097–2102.

[41] M. Bernard, K. Kondak, and G. Hommel, "A slung load transportation system based on small size helicopters," in *Autonomous Systems – Self-Organization, Management, and Control*, B. Mahr and S. Huanye, Eds. Dordrecht: Springer Netherlands, 2008, pp. 49–61.

[42] P. Kirienko, "Opengrab epm v3 knowledge base," see: Safety note under mechanical properties, Accessed: 12-10-2019. [Online]. Available: https://kb.zubax.com/display/MAINKB/OpenGrab+EPM+v3

[43] Y. Feng, C. A. Rabbath, and C.-Y. Su, *Modeling of a Micro UAV with Slung Payload*. Dordrecht: Springer Netherlands, 2015, pp. 1257–1272. [Online]. Available: https://doi.org/10.1007/978-90-481-9707-1_108

[44] Robot Shop, "Hc-sr04 ultrasonic sensor working," accessed: 12-16-2019. [Online]. Available: https://www.robotshop.com/uk/hc-sr04-ultra01-ultrasonic-range-finder.html

[45] TSKTECH, "Inductive proximity sensor," accessed: 12-16-2019. [Online]. Available: https://www.amazon.in/INDUCTIVE-PROXIMITY-SENSORS-SWITCH-Printer/dp/B07BJHXMBB

[46] Electronics-Tutorials, "Mosfet as a switch," accessed: 12-12-2019. [Online]. Available: https://www.electronics-tutorials.ws/transistor/tran_7.html

[47] V. Walter, T. Novák, and M. Saska, "Self-localization of unmanned aerial vehicles based on optical flow in onboard camera images," in *Modelling and Simulation for Autonomous Systems*, J. Mazal, Ed. Cham: Springer International Publishing, 2018, pp. 106–132.

[48] P. Stepan, T. Krajnik, M. Petrlik, and M. Saska, "Vision techniques for on-board detection, following, and mapping of moving targets," *Journal of Field Robotics*, vol. 36, no. 1, pp. 252–269, 2019. [Online]. Available: https://onlinelibrary.wiley.com/doi/abs/10.1002/rob.21850

[49] V. Spurny, T. Baca, M. Saska, R. Penicka, T. Krajnik, J. Thomas, D. Thakur, G. Loianno, and V. Kumar, "Cooperative Autonomous Search, Grasping and Delivering in a Treasure Hunt Scenario by a Team of UAVs," *Journal of Field Robotics*, vol. 36, no. 1, pp. 125–148, 2019.

[50] T. Baca, P. Stepan, and M. Saska, "Autonomous landing on a moving car with unmanned aerial vehicle," in *The European Conference on Mobile Robotics (ECMR)*, 2017.

[51] T. Baca, D. Hert, G. Loianno, M. Saska, and V. Kumar, "Model predictive trajectory tracking and collision avoidance for reliable outdoor deployment of unmanned aerial vehicles," in *2018 IEEE/RSJ International Conference on Intelligent Robots and Systems (IROS)*, Oct 2018, pp. 6753–6760.

[52] Supermagnete, "Shear force on magnet faqs," accessed: 12-19-2019. [Online]. Available: https://www.supermagnete.de/eng/faq/Why-does-my-magnet-not-carry-the-maximum-weight-on-the-wall

Appendices

CD Content

In Table 1 are listed names of all root directories on CD.

Directory name	**Description**
thesis	This thesis in PDF format
thesis_source	Latex source code and figures used
source_codes	Latest version of the gripper firmware running on the MCU and the ROS node
models	STL/design files of gripper for 3D printing
videos	videos of conducted experiments

Table 1: CD Content

List of abbreviations

In Table 2 are listed abbreviations used in this thesis.

Abbreviation	Meaning
ADC	Analog-Digital Converter
COTS	Commercial Over the Shelf
DC	Direct Current
DOF	Degree of Freedom
EPM	Electro-Permanent Magnet
ESC	Electronic Speed Controller
GPS	Global Positioning System
IDE	Integrated Development Environment
I/O	Input/Output
LIDAR	Light Detection and Ranging
MBZIRC	Mohammed Bin Zayed International Robotics Challenge
MCU	Microcontroller Unit
MRS	Multi-Robot System
MOSFET	Metal Oxide Semiconductor Field Effect Transistor
RPM	Revolutions Per Minute
ROS	Robot Operating System
UART	Universal Asynchronous Receiver-Transmitter
UAV	Unmanned Aerial Vehicle
UGV	Unmanned Ground Vehicle
USB	Universal Serial Bus
WIFI	Wireless Fidelity
VTOL	Vertical Take-Off & Landing

Table 2: Lists of abbreviations